Chapter 3
Groundwater Engineering Problem and Prevention

During the survey, design and construction of underground engineering, groundwater is always the very crucial issue. It directly affects the properties and behaviors of rock and soils as a part of component of them, as well as some kind of underground construction environment, it also has great influence on the stability and durability of engineering projects. In design, full account must be taken on the various roles of geotechnical and underground engineering. All kinds of potential environmental geological problems which may rise due to groundwater during construction should be also paid much attention to take some appropriate preventive measures.

3.1 Adverse Actions of Groundwater

3.1.1 Suffosion

Suffosion is a kind of undermining phenomenon through removal of sediment by mechanical and corrosional action of groundwater flow. Usually, it is described the process of removal and transport of small soil particles through pores resulted in underlying caves or voids.

3.1.2 Pore-Water Pressure

In saturated soils, any small tiny variation of stress will change the pore pressure conditions. It always influences the strength, deformation of soils and stability of engineering projects, such as slope stability problem, deep foundation pit excavation in high-rise building projects, etc.

Y. Tang et al., *Groundwater Engineering*, Springer Natural Hazards,
DOI 10.1007/978-981-10-0669-2_3

3.1.3 Seepage Flow

When water flows horizontally through an aquifer, the flow undergoes a reduction of pressure head because of friction. Thus the pressure on the upstream side of a small element is larger than on the downstream side. The water then exerts a net force on the aquifer element. The net force in the flow direction is the seepage force.

If there is an upward vertical flow, the head loss due to friction as the water flows into the pores results in an increase in the hydrostatic pressure. This in turn results in a decrease of the intergranular pressure. A point can be reached when the upward seepage force is large enough to carry the weight of the sand grains so that the sand or silt behaves like a liquid. It has no strength to support any weight on it. This condition is known as quicksand.

3.1.4 Uplift Effect of Groundwater

Groundwater has hydrostatic water pressure on the rock or soil mass below water level, which is resulted in buoyancy. From Archimedes' principle, the upward buoyant force exerted on a body immersed in a fluid is equal to the weight of the fluid the body displaces, i.e., when the water in soil pore spaces or fractures and voids in rock has hydraulic connection with groundwater, the buoyant force is buoyancy of rock mass or soil particle volume, which is the weight of displaced fluid.

3.2 Suffosion

3.2.1 Types of Suffosion

3.2.1.1 Mechanical Suffosion

Under the action of seepage force, particles of soil or rock mass are removed away from pore voids or caves by groundwater.

3.2.1.2 Chemical Suffosion

Groundwater dissolves the soluble substances in soil, breaks the cementing and weakens binding force among soil particles and thus makes soil structure loose. Generally, mechanical and chemical suffosion occur simultaneously. The chemical action takes away the soluble materials through groundwater flow leaching, which provides the circulation condition for mechanical suffosion. Suffosion actions reduce the strength of foundation soils and even form underground caves, thus results in surface subsidence and adversely affect the stability of buildings. Suffosion is greatly linked to karst terrain development and loess area and is accompanied by widespread collapse.

3.2.2 Conditions of Suffosion

It is involved in two aspects, i.e., first soil composition and second the sufficient hydrodynamic conditions. The specific details are depicted as follows:

(1) When the coefficient of uniformity ($C_u = \frac{d_{60}}{d_{10}}$, d_{60}, d_{10} are the particle-size diameters corresponding to 60 and 10 %, respectively) is large, resulting in high potential in suffosion, and specifically as $d_{60}/d_{10} > 10$.
(2) Soils with interface layers: when the permeability ratio $K_1/K_2 > 2$, suffosion is greatly conducive to occur in the interface.
(3) The hydraulic gradient. When it approaches to 5 ($I > 5$), the groundwater flow in turbulent condition facilitates suffosion. As a matter of fact, so large hydraulic gradient would rarely happen, hence a critical hydraulic gradient I_c is proposed out based on engineering practice:

$$I_c = (G_s - 1)(1 - n) + 0.5n \tag{3.1}$$

where G_s is the specific gravity, N/m^3; n is the porosity, expressed as a decimal.

3.2.3 Prevention of Suffosion

The measurements are mainly focused on following points:

(1) Reinforce the soils (e.g., grouting);
(2) Artificially lower the groundwater hydraulic gradient level;
(3) Set the filter layer.

Filter layer is a protecting measurement to prevent suffosion. It can be placed in the seepage exposure, especially directly at the exit point of the seepage. It is always composed of ranges of sizes of non-cohesive particles. Usually, these layers are arranged perpendicularly to the seepage lines and in sequence of increasing particle size (Fig. 3.1). It is extremely important to choose appropriate particle sizes when designing the filter to protect soils in place. Even when soils under really high hydraulic gradient (I = 20 or larger) can be protected well if the filter works effectively. Generally, the filter is designed into three layers, sometimes two layers

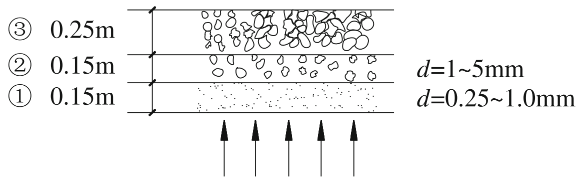

Fig. 3.1 Filter structure

as well, with thickness of 15–20 cm in each. How to control the specific thickness of each layer mainly depends on the construction conditions and the particle size used in this layer. If the filter layer could not be placed evenly or the quality could not meet the requirement, the thickness should enlarge to ensure that filter failure would not happen.

3.3 Piping and Prevention

3.3.1 Piping

The term "piping" is usually applied to a process that starts at the exit point of seepage and in which a continuous passage or pipe is developed in the soil by backward erosion, and enlarged by piping erosion. When soils around or beneath the foundation pit are loose sandy layers, if the seepage forces exerted on foundation soil are large enough and the pore spaces are large enough, water that percolates through earth dams or foundations can carry away fine soil particles. At the same time the pore spaces are also enlarged and a passage or pipe along seepage path is gradually developed through foundations or earth dams. Thus the foundation soils or earth dam soils are emptied continuously finally resulting in instability or failure. This phenomenon is namely piping. The specific process is shown in Fig. 3.2.

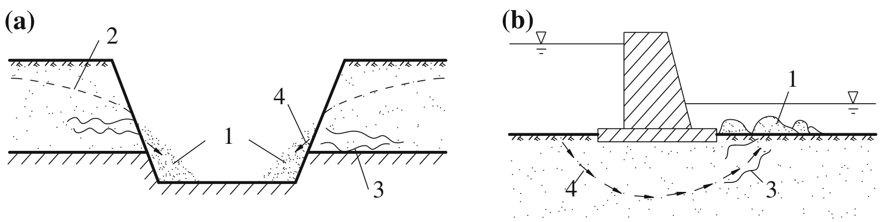

Fig. 3.2 Piping failure schematic under different conditions: **a** Slope soils; **b** Foundation soils; *Note 1* packing particle during piping; *2* groudwater level; *3* piping passage; *4* seepage direction

Scholars all over the world have studied piping extensively. Numbers of computation methodologies are figured out. A simple and practical assessment method is introduced here.

When the conditions shown as Eq. (3.2) can be met, the foundation pit is stable. The possibility of piping occurrence will be rarely small.

$$I < I_c \tag{3.2}$$

where I is the hydraulic gradient in situ, it can be calculated by:

$$I = \frac{h_w}{l} \tag{3.3}$$

I_c is the critical hydraulic gradient, in can be calculate by:

$$I_c = \frac{G_s - 1}{1 + e}; \tag{3.4}$$

h_w is the hydraulic head difference between outside and inside of retaining wall, m; l is the shortest length of flow line, m; G_s is the specific gravity, N/m^3; e is void ratio.

3.3.2 Conditions of Piping

Piping generally happens in sandy soils. It is characterized by poor uniformity (gap-graded soil), i.e., some particle sizes are missing and pore void is large and well connected. It is mostly composed of low specific gravity minerals, which can be easily washed away by water percolating. In addition, good seepage exit path is also another sufficient condition for piping failure. All the above can be expressed specifically as following:

(1) The ratio of coarse and fine particles is larger than 10: $D/d > 10$;
(2) The coefficient of uniformity of the soil is larger than 10: $C_u = d_{60}/d_{10}$;
(3) The permeability ratio of two interface layers is greater than 2–3: $K_1/K_2 > 2–3$;
(4) The hydraulic gradient of seepage is greater than critical hydraulic gradient.

3.3.3 Prevention of Piping

(1) Increasing the embedded depth of retaining structure. As shown in Fig. 3.3, the length of flow lines can be extended and resultantly the hydraulic gradient is reduced. This is favorable to prevent piping.

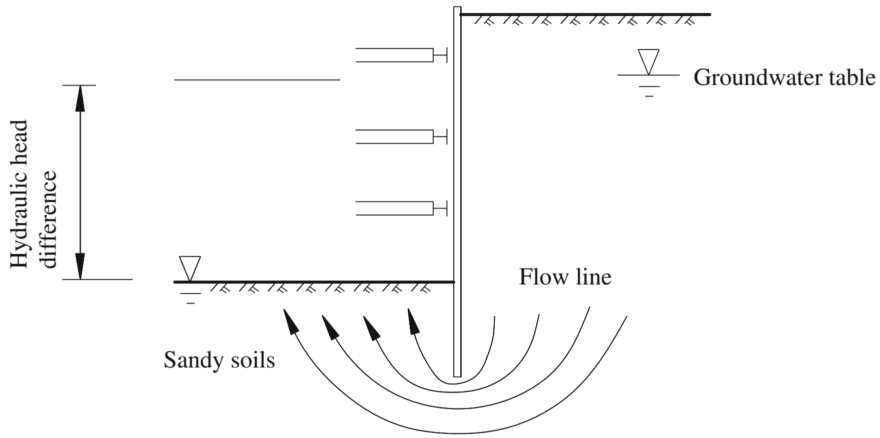

Fig. 3.3 Piping in foundation pit

(2) Artificially lowering the groundwater level and changing the groundwater seepage direction. When the foundation soils are sandy layers, and the seepage force is upward, the foundation pit underside will heave if the hydraulic gradient is greater than the critical hydraulic gradient in this condition.

To prevent this piping phenomenon (shown in Fig. 3.3), the embedded depth should be increased or artificially dewatering to lower the groundwater level before any construction.

3.3.4 Case Study

In this project, the bottom of this foundation pit is 6.5 m below the ground level, with 12 m in width and 1:1.25 slopes at both sidewalls. The foundation soils are clay layers with interbedded sand layers (Fig. 3.4). Grade 2 light wellpoint of

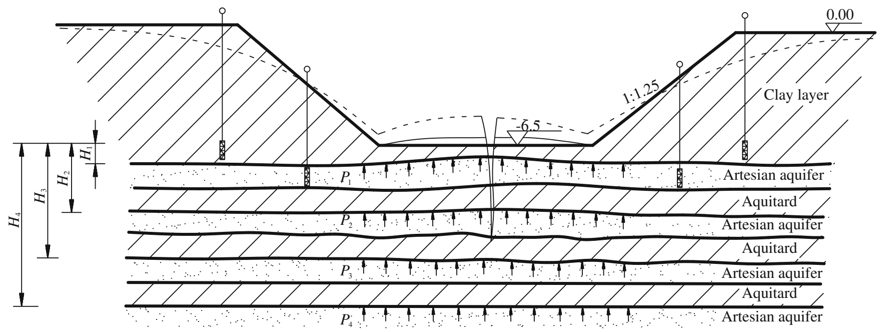

Fig. 3.4 Schematic of piping caused by foundation pit construction

dewatering is used here. When the foundation pit was dig excavated into the designate depth, the bottom heave gradually occurred. Firstly 20 cm in the center of bottom happened after 24 h. It reached up to 30 cm after another night. After 3 days, the accumulated heave is high as 1.5 m. At the beginning of heave in the pit bottom, no piping phenomenon was investigated. It happened until the heave reached a large amount finally. During the heaving, the slope and top correspondingly sunk and slid toward foundation pit.

Analysis of the reasons: the designated depth of wellpoint system was not deep enough. The water pressure in the artesian aquifer layers beneath the foundation pit was larger than self-weight of overlying layers. The clay layer in the pit bottom was uplifted and cracked, then piping happened.

Measurements: The dewatering system should be embedded into nth artesian aquifer layer, in which the water pressure in this artesian aquifer layer should be smaller than the total self-weight of overlying layers, i.e., $P_n < \sum_{i=1}^{n} H_i \cdot \gamma_i$, where H_i is the soil thickness of nth layer; γ_i is the bulk weight of nth layer.

3.4 Quicksand and Prevention

3.4.1 Quicksand

Quicksand is saturated loose sand or silty sand (including sandy silt and clayey silts as well) in the case of upward flowing water, seepage force opposes the force of gravity and suspends the soil particles. This creates liquefied soil that forms suspension and lose strength. Quicksand usually happens in uniformly graded fine or silty sands; it sometimes occurs in silts as well. The saturated sediment may appear quite solid until a sudden change in pressure or shock initiates liquefaction. All the fine particles are washed away suddenly by percolating water. Resultantly, sliding or differential subsidence occur in foundation, even worse to collapse or suspension. As shown in Fig. 3.5, quicksand happens in unexpected sudden. It is really harmful to engineering practice.

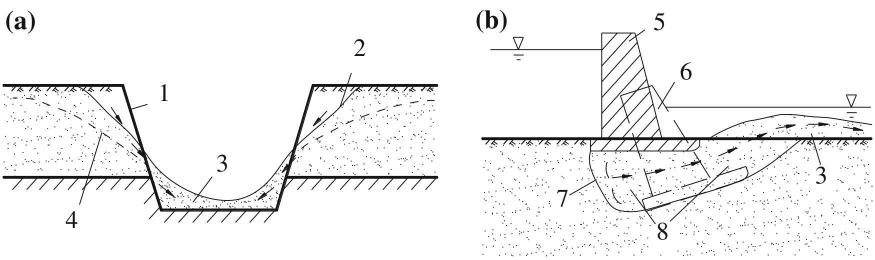

Fig. 3.5 Quicksand failure. **a** Slope soils; **b** Foundation soils, *Note 1* original slope; *2* the slope surface after quicksand occurrence; *3* quicksand packing particles; *4* groundwater level; *5* original position of structure; *6* the position after quicksand occurrence; *7* sliding surface; *8* quicksand area

3.4.2 Causes of Quicksand

(1) Large hydraulic gradient and high flow velocity make the fine particles suspense;
(2) Quicksand usually is a colloid hydrogel consisting of fine granular materials (such as sand or silt), clay and water. When saturated soil particles absorb water and swell and the density is reduced a lot. Thus it can be suspended easily by water percolating.
(3) Sand structure is destroyed by sudden vibration. In this case the vibrated force immediately increases the pore pressure of groundwater. The saturated sand loses strength and suspends away with water flow.

In practice, when a pit excavation is conducted below the groundwater level, sands with groundwater spring out frequently. This phenomenon is namely boiling sand (Fig. 3.6a). Sands spring out more serious when excavation is advancing. Quicksand brings great difficulties to construction, and also destroys the foundation strength; threaten the safety of surrounding existed buildings. This phenomenon can be explained in this simple model test. In Fig. 3.6, first open valve A to make an upward water stream in sand. When the upward hydraulic gradient was greater than 1, i.e., $I = h/l \approx 1$, the sand lose the stability. The gravel on the sand surface sunk (the sand lost the strength). Then close the valve, the sand would gain its strength again.

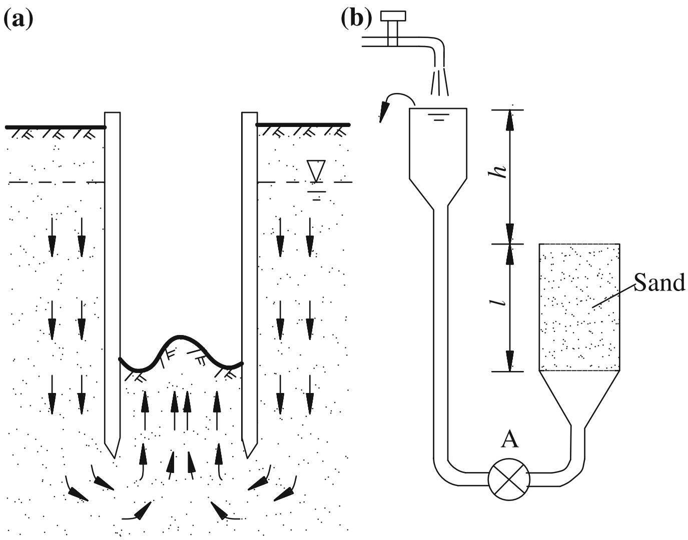

Fig. 3.6 Quicksand modeling tests

3.4.3 Conditions of Quicksand

(1) Large hydraulic gradient. The seepage force exceeds the particle gravity and makes the fine suspension;
(2) The sand has large porosity. The larger, the easier to form quicksand;
(3) The sand has poor permeability. The poorer, more favorable to quicksand;
(4) Composed of more platy minerals, such as mica, chlorite, the sand is more potential to quicksand.

The influence factors and distribution of quicksand in Shanghai area is preliminarily figured out based on borehole data and geotechnical soil tests. These factors are shown as follows:

(1) The main induced external factor depends on the groundwater hydraulic head difference. With the excavation depth is increasing, the hydraulic head difference gets larger, quicksand is much easier to happen;
(2) The particle composition. In this case, the clay percentage is smaller than 10 %, while silt and sand total content is over 75 %;
(3) The coefficient of uniformity is smaller than 5. From quicksand properties data of in situ engineering projects, mostly the coefficient of uniformity is in the range of 1.6–3.2;
(4) The water content is greater than 30 %;
(5) The porosity is larger than 43 % (or void ratio is larger than 0.75);
(6) When sand soils interbedded into clay layers, the thickness of sandy soil or clayey silt should not be over 25 cm;

There are also some similar assessment standards in practical area outside China: natural porosity is greater than 43–45 % (void ratio larger than 0.75–0.80), effective particle size is smaller than 0.1 mm ($d_{10} < 0.1$ mm), and the coefficient of uniformity is smaller than 5 ($C_u < 5$), the soils have these characteristics are easier to happen quicksand.

In Shanghai area, when the water level is around 0.7 m below the ground surface, and the excavation depth is greater than 3 m, meantime the soil has properties described above; quicksand has great potential to happen. When the excavation depth is smaller than 4 m, usually sheet piles are used to excavation. When the excavation depth is over 4 m, dewatering of wellpoint system should be used.

3.4.4 Determination of Quicksand

The phenomenon of quicksand encountered in constructions:

(1) Slight—there is minor gap between sheet piles. Some sands move into the foundation pit through the gap by percolating water and make the pit much muddier;
(2) Moderate—close to the foundation pit bottom, especially nearby the sheet piles, usually there are packing fine sand particles slowly spring out. Investigated closely, it can be founded that a lot of small seepage exits in the packing sands and the water bubbles up with fine particles.
(3) Severe—if the above phenomenon happened during excavation and no measurements were taken to control and still kept excavating. In this case, the quicksand velocity would increase fast and finally formed boiling sands. At this time the sands at the pit bottom would liquefy and flow.

In Shanghai area, there are a lot of quicksand cases, such as before the People's Republic of China established, on Fujian Seven Road of Shanghai, there was a quicksand during the ditch construction. The liquefaction at the pit bottom was really serious and workers used barrels as tool to move sands and water. Another example is the pumping station construction in Shanghai Yejiazhai Road. At that time the excavation depth was very large but the embedded depth of sheet piles was not deep enough. Server quicksand happened at the lower part of the ditch. Soils at the bottom totally liquefied. All these stopped the progress of construction and made the ditch tube could not reach the designated depth and changed it as 60 cm higher. From Fig. 3.7, it is shown the quicksand circumstance during the narrow and long ditch construction. This phenomenon was also influenced by hydraulic head difference, while under the upward flow effect, closer to the edge of the sheet pile walls, more serious quicksand happened. Meantime, in practical construction land subsidence nearby sheet pile area always occurred. The ditch width was very small; the water in the surrounding soils of the ditch area flew to the ditch and concentrated at the pit bottom. Thus closer to the sheet pile walls, the flow velocity was faster. The water flux per length along the ditch can be evaluated by Eq. (3.5):

$$q = bKI, \tag{3.5}$$

Fig. 3.7 Quicksand around the sheet pile during excavation

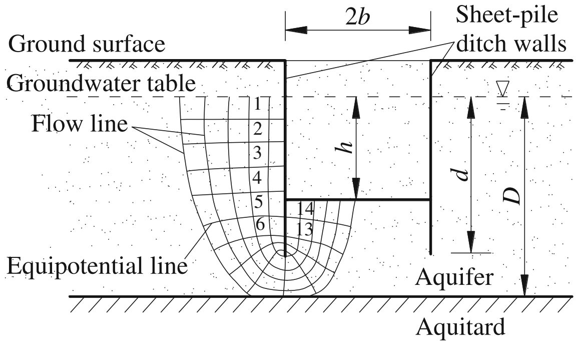

Table 3.1 The reduction factor

d/D	0.1	0.2	0.3	0.4	0.5	0.6	0.7	0.8	0.9	1.0
Reduction factor for q (%)	5	10	15	20	25	30	40	50	65	100

where q is the water flux, m^2/s; b is half of the ditch width, m; K is the hydraulic conductivity of surrounding soil, m/s; I is the hydraulic gradient.

The above Eq. (3.5) can only be used when the embedded depth of the sheet pile wall d is really small corresponding to the aquifer thickness D. If the embedded depth is very deep, the results should multiply to a reduction factor. As for the reduction factor value, it is shown in Table 3.1.

When calculating the embedded depth of sheet piles, besides the critical value obtained from Eq. (3.4), flow net methodology is still needed for calculation. And in practice, safety factor should be considered to be greater than 1, since in soils with good permeability the fine particles can be easily moved. In clay and silty clay, the seepage discharge is really small or even could not occur. Quicksand can hardly happen in these conditions. And in gravel, good permeability and large discharge amount, the seepage path is very long. Thus quicksand rarely happens as well. Hereby quicksand mostly happens in fine or silty sands with poor permeability. The fine sands or silts can easily lose strength with high seepage force exerted on; and moved by percolating water to ditch pit. Therefore, when excavation in this kind of soil, effective measurements should be taken during construction to avoid quicksand happening.

Example:

A ditch was constructed by sheet piles (Fig. 3.7). The specific gravity of the aquifer sand G_s is 2.8; the void ratio is 0.8; and γ_w = 1 g/cm^3, h = 21 m. There are 14 flow paths in the flow net (n = 14). The length can be selected as 1 along the ditch. Is this project reach quick condition?

Solution:

From Eq. (3.4), $I_c = \frac{G_s - 1}{1 + e} = \frac{2.8 - 1}{1 + 0.8} = 1$,

From drawing flow net, $I = \frac{h}{n \times L} = \frac{21}{14 \times 1} = 1.5 > 1$,

Hence, quicksand will happen in natural condition.

3.4.5 Quicksand in Foundation Pit

Figure 3.8 presents the schematic of quicksand calculation. Due to the water level difference h' existed in the ditch around the foundation pit, a seepage flow runs down through the soils outside the sheet piles, and when it flows over the end of the sheet piles, the water advances up reaching the bottom of the pit, which is collected into the well by the ditch. Finally, all the water is pumped away. Hence, the soils beneath the pit are saturated by water and the effective unit weight γ' should be used in calculation. When the value of unit seepage force or hydrodynamic pressure G_D

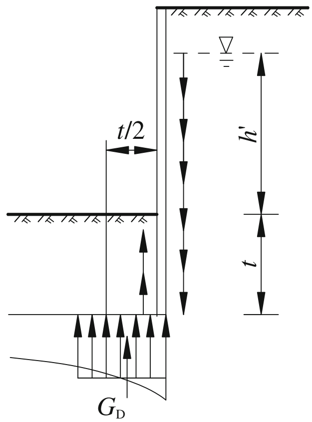

Fig. 3.8 The seepage during the construction of foundation pit

is equal to or even over the effective gravity γ', the soil particle is under a state of quicksand and is able to move free with water flow. To avoid this adverse phenomenon, the requirement as below should be met.

$$\gamma' \geq K_s G_D \tag{3.6}$$

where K_s is the safety factor, it depends on the retaining structure and soil properties; generally, K_s = 1.5–2.0.

According to the relevant experiment results, quicksand initially occurred within the distance of $t/2$ (t is the embedded depth of sheet pile wall) to the sheet pile wall. And the location closest to the sheet piles has the shortest seepage path and the largest seepage force can be calculated as below.

$$G_D = I \cdot \gamma_w = \frac{h'}{h' + 2t} \cdot \gamma_w$$

In conjunction with Eq. (3.6), the above condition can be changed into $\gamma' \geq K_s \frac{h'}{h' + 2t} \cdot \gamma_w$.

After some transposition operation, the specific requirement for the embedded depth of sheet pile wall is calculated as Eq. (3.7).

$$t \geq \frac{K_s h' \gamma_w - \gamma' h'}{2\gamma'} \tag{3.7}$$

If the soil layers above the bottom surface of the foundation pit are coarse gravel, loose fill soil or fractured soil, the head loss in the soil layer outside the foundation pit can be neglected, so Eq. (3.7) can be simplified as

$$t \geq \frac{K_s h' \gamma_w}{2\gamma'}$$

or

$$K_s \leq \frac{2\gamma' t}{h' \gamma_w} \quad (3.8)$$

where h'/t is the hydraulic gradient in the soil outside the sheet pile wall. The increase of h'/t will result smaller K_s. When K_s less than 1, quicksand will happen. The value of h'/t as $K_s = 1$ is called limited hydraulic gradient. In the designation of embedded depth of sheet pile wall, the value of K_s should be chosen as 1.2–1.5.

3.4.6 Quicksand in the Caisson

During the construction of caisson in sands, if drainage sinking is used and the dewatering depth is not large enough or the dewatering is not effective, quicksand will easily happen in the sands beneath the caisson cutting edge under hydrodynamic pressure, shown as Fig. 3.9. Some ground subsidence and horizontal displacement maybe concomitantly occur.

During the undrained sinking of the open caisson in sands, if the water level inside the caisson is much lower than the outside, large hydrodynamic pressure is generated and results in quicksand in the bottom of the caisson. And surrounding soil movement will occur as well.

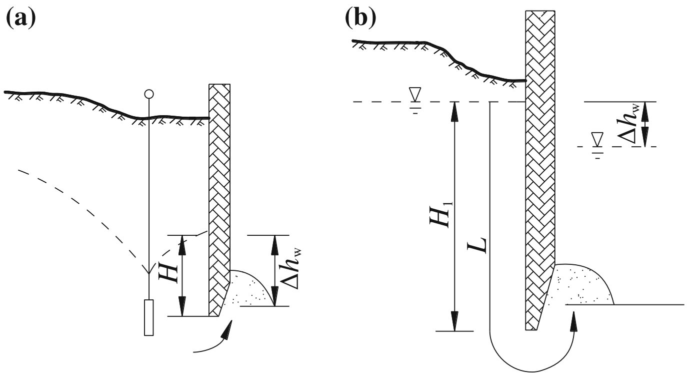

Fig. 3.9 The soil movement induced by quicksand in open caisson: **a** The depth of open caisson is not enough during drained sinking. **b** The head difference is very large during undrained sinking

The influence range can be extended (1–3) H around the caisson (H is the caisson depth). The ground subsidence amount usually depends on the soil water loss. Long-time soil water loss will induce catastrophic ground subsidence. It should be noted here, when the sands is overlying by hard clay layer, large-area collapse is probably to happen as the underlying sands is continuously removing due to quicksand.

Quicksand happening in the caisson will influence the nearby shallow foundation constructions and also the pile foundation buildings. When conducting the caisson construction in the saturated sands near some pile foundation, pile displacement and inclination may be attributed to the surrounding soil movement toward the caisson bottom during the caisson sink, rather than the soil consolidation by well dewatering. If quicksand does happen in the caisson bottom, large movement will arise in surrounding soils. Even nearby is deep foundation construction, it can be damaged greatly.

3.4.7 The Prevention and Treatment of Quicksand

As mentioned above, when the hydrodynamic pressure exceeds the buoyant (submerged or effective) unit weight or the hydraulic gradient is larger than the critical value, quicksand is probably to happen. This circumstance is usually induced by the excavation beneath ground water, the laying of underground pipes, well construction, etc. Hence, quicksand is an engineering phenomenon. It can cause large soil movement and result in ground collapse or building foundation damage. Significant difficulties can be brought into the construction, and direct influence to surrounding construction project and building stability maybe emerge. Therefore, necessary prevention and treatment should be paid attention.

In the potential quicksand area, it had better conduct in the overlying soil layer as natural soil foundation, or use pile foundation through the whole quicksand area transferring the upload into stable soil layer. In total, the excavation should avoid the quicksand area. If it could not be avoided, several treatments can be utilized as below.

(1) Artificially dewater the groundwater level to ensure it below the quicksand layer, shown in Fig. 3.10.

The prevention principle:

During the excavation, a upward seepage force is exerted on soils below the surface. As for sands, when the hydraulic gradient increases to some extent, quicksand will happen, i.e., the soil flow out of slope surface akin to a liquid state. The limited seepage hydraulic gradient inducing quicksand can also use the critical hydraulic gradient proposed by Terzaghi.

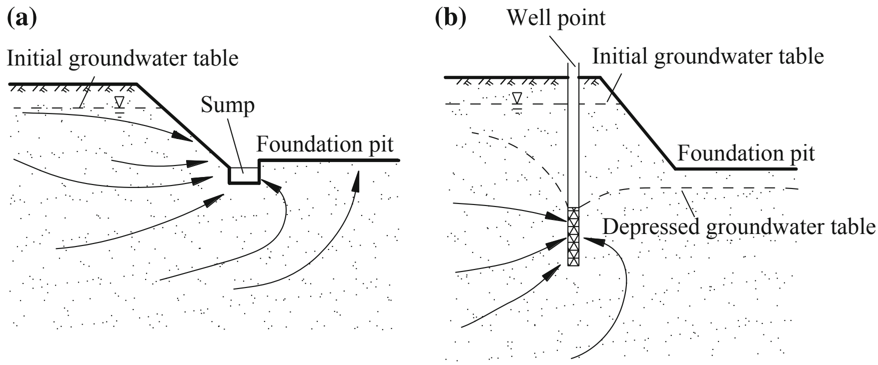

Fig. 3.10 Prevention of quicksand by well dewatering. **a** Sump **b** Well point

Fig. 3.11 The seepage force in the foundation pit

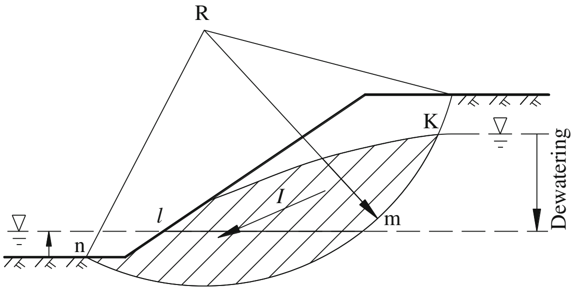

$$I_c = (1 - n)(G_s - 1) \tag{3.9}$$

where n is the porosity; G_s is the specific gravity of soil particle.

As for uniform sand soils, I_c = 0.8–1.2. In practice, some safety factors will be used in designation. As for the nonuniform silty sands, the critical hydraulic gradient can only be I = 1/3. If the hydraulic gradient exceeds the design allowable value, well dewatering should be conducted to prevent the quicksand phenomenon. The well dewatering declines the seepage head difference existing inside and outside the foundation pit, and indirectly control the hydraulic gradient within the allowable value, shown as Fig. 3.11. Simply only drainage ditch could not lower the seepage hydraulic gradient. Dewatering well cannot only decrease the hydraulic gradient within the safe value, but also change the seepage flow direction, which make the water flow moves into dewatering well pipe.

(2) Sheet pile wall can be constructed. This method has advantages in two aspects. First it can reinforce the foundation pit as retaining wall; second it prolongs the seepage path so that to decline the hydraulic gradient and slower the seepage velocity.

(3) Artificial ground freezing. This method can be used before excavation. Surrounding soils are frozen as a water-sealing wall with higher strength.

(4) Excavation in submerged condition. To avoid quicksand induced by head difference from drainage and to strengthen the stability of sands, the excavation can be performed whilst injecting (recharging) water into the foundation pit.

In addition, some other methods such as chemical reinforcement, blasting method, strengthen weighting, etc. When some local quicksand occurs during excavation, filling coarse gravel can alleviate the quicksand movement greatly.

3.5 Liquefaction of Sands and Relevant Preventions

3.5.1 Liquefaction

A number of failure of embankment, natural slopes, earth structures and foundations have been attributed to the liquefaction of sands caused by either static or seismic loading. The liquefaction phenomenon of soil deposits can be described as the reduction of shear strength due to pore pressure buildup in the soil skeleton. When some saturated loose sand (including some silt) is applied by vibration load or a static load sharply, if the pore water could not flow out in time, the contractancy of loose sands is responded in continuously increasing of pore-water pressure. Correspondingly, the effective stress σ' gradually decreases. When $\sigma' = 0$, the saturated soil substantially loses shear strength and stiffness. At the onset of initial liquefaction, loose sands will undergo unlimited deformations or flow without mobilizing significant resistance to deformation. As a result, structures supported above or within the liquefied deposit undergo significant settlement and tilting; water flows upward to the surface creating sand boils; and buried pipelines and tanks may become buoyant and float to the surface. This is usually termed as liquefaction.

The phenomenon of liquefaction is most often observed in any part of saturated loose sands. It can occur in the ground surface, or some depth underground, depending on the sand condition and vibration circumstance. Sometimes the shallow sand layers are liquefied induced by liquefaction of underlying sands. The excess pore-water pressure is dissipated by upward flowing of water. If the hydraulic gradient is so large that the upward water flow may destroy the stability of overlying sand layers and results in seepage failure. Even the failure has not shown up but the strength of overlying sand layers will be lowered severely.

Usually phenomena of sand boils, water spouts, and ground cracks appear in the areas of liquefaction. The waterspouts can reach as high as several meters and the sand concomitant accumulates as a crateriform around the spray spout in a diameter of several meters. These mostly start to happen several seconds shortly after a strong earthquake arises, and lasts decades' minutes to a few hours after the earthquake stops, or even tens of hours. However, sand boils and water spouts may not always happen in some circumstances, such as when the liquefaction sensitive sand layers are deep beneath the ground surface with very thin thickness. The upward spraying pore-water and sand particles are not sufficient to reach the ground surface. Just some sand veins are formed in the overlying layers. This kind potential liquefaction in deep soil usually will not cause tremendous amount of damage.

Liquefaction of sands induces to lose the bearing capacity and some concomitant movements. It always brings a lot of catastrophic failure and damage. Case histories of landslides or flow failures due to liquefaction are the 1937 Zeeland coast of Holland slides involving 7 million cubic meters of alluvial sands, and the 1944 Mississippi River slid near Baton Rouge containing about 4 million cubic meters of fine sands. Failures of hydraulic fill dams such as the Calaveras Dam in California in 1918, the Fort Peck Dam in Montana in 1938, and the Lower San Fernando Dam during the 1971 San Fernando Earthquake in California, just to name a few, were triggered by the liquefaction of sands. Although the importance of liquefaction of sands induced by static loading has been recognized since the work of Casagrande (1936), the subject of liquefaction of sands by seismic loading had not received a great deal of attention until 1964 when two major earthquakes shook Anchorage, Alaska, and Niigata, Japan, resulting in substantial damage and loss. The Alaska earthquake in 1964, a shock with a magnitude, M, of 9.2 on the Richter scale, destroyed or damaged more than 200 bridges and caused massive landslides. Moreover, the 7.5-magnitude earthquake of June 16, 1964, in Niigata, Japan, the extensive liquefaction of sand deposits resulted in major damage to buildings, bridges, highways and utilities. Foundations lost the bearing capacity and engineering constructions damaged severely. Over 1 meter settlement occurred in most areas. Several apartments tilted almost 80°. During the liquefaction, some groundwater spouted out from the ground cracks. Meanwhile, cars, buildings, or other objects on the ground surface sunk into underground soils. And some underground constructions damaged and were risen up to the ground surface. Some harbor port facilities were damaged a lot. It was estimated that more than 60000 buildings and houses were destroyed.

There were subsequent 229 disasters of sand liquefaction near Southwest Seaside in Netherlands in 1861–1947. The influence area was as high as 2.5 million square meters. The liquid soils in movement reach 25 million cubic meters. The original coast slope was 10°–15°, and was decreased as 3°–4° after liquefaction. A reservoir in Xinjiang, with a 3.5–7.1 m height dam, was established in 1959. In April 1961, a 9° strong earthquake occurred here and in October 1962, the second earthquake happened again. The sandy silts (just tens of centimeters in thickness) were liquefied and the dam was slid and resulted in dam foundation damage. At the 8° earthquake area in Xingtai in 1966, sands spouted out from ground cracks and hydraulic gate of dams were mostly lower down. From the Tangshan earthquake, there were four kinds of liquefaction. Flat sheeted and striped liquefaction were distributed in the view of surface (Fig. 3.12). Shallow soil and deep soil liquefactions were observed from the view of vertical profile. The sheeted liquefaction and shallow liquefaction arose in the alluvial fan areas of the river. Striped liquefaction and deep soil liquefaction mostly occurred in the downstream of the ancient river. The damage differed in these various distributions. Specific analysis on the soil distributions can make great significance to ensure more applicable designation.

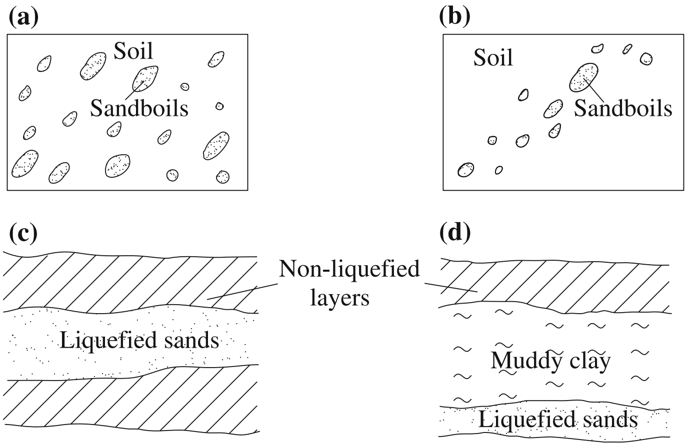

Fig. 3.12 Liquefaction properties (from Handbook of design and construction of underground engineering, 1999). **a** Sheeted liquefaction surface; **b** Striped liquefaction surface; **c** Shallow soil liquefaction; **d** deep soil liquefaction

From the statistical investigation of earthquake damage, more than half of the earthquake damages are induced by liquefaction. Taking Hatching Earthquake and Tangshan Earthquake as examples, the number of building failures due to foundation liquefaction accounted for almost 54 % of the total foundation damages. Foundation liquefaction can make the buildings tilt, collapse, or induce ground uplift, cracks, or slides of coast slope surface. Some shallow light construction (such as pipes) can be moved upward to ground surface as well. In total, all the facilities in the liquefaction area can hardly avoid the damage.

However, it is worth remarking that once liquefaction happens, the above various damages will arise but the surface movement can be alleviated. Since the liquefaction layer can effectively weaken the energy transfer of upward shear wave. At the same time the accompanied sand boils and waterspouts can consume a part of energy and results in smaller energy reaching the ground surface. Hence the vibration duration can be shortened. This is the reason that the seismic intensity in the liquefaction area is always not higher than nonliquefaction area, even smaller. Acknowledge of the advantages and adverse aspects of liquefaction in earthquake disaster is very important for improving the aseismic design level. In practice, firstly whether the foundation is sensitive to liquefaction or not should be distinguished. Then the relevant measurement can be adopted.

3.5.2 The Factors Affecting Liquefaction

From the statistical investigation of earthquake damage, more than half of the earthquake damages are induced by liquefaction. Taking Hatching Earthquake and

Tangshan Earthquake as examples, the number of building failures due to foundation liquefaction accounted for almost 54 % of the total foundation damages. Foundation liquefaction can make the buildings tilt, collapse, or induce ground uplift, cracks, or slides of coast slope surface. Some shallow light construction (such as pipes) can be moved upward to ground surface as well. In total, all the facilities in the liquefaction area can hardly avoid the damage.

However, it is worth remarking that once liquefaction happens, the above various damages will arise but the surface movement can be alleviated. Since the liquefaction layer can effectively weaken the energy transfer of upward shear wave. At the same time the accompanied sand boils and waterspouts can consume a part of energy and results in smaller energy reaching the ground surface. Hence the vibration duration can be shortened. This is the reason that the seismic intensity in the liquefaction area is always not higher than nonliquefaction area, even smaller. Acknowledge of the advantages and adverse aspects of liquefaction in earthquake disaster is very important for improving the aseismic design level. In practice, firstly whether the foundation is sensitive to liquefaction or not should be distinguished. Then the relevant measurement can be adopted.

Based on field observation and laboratory testing results, liquefaction characteristics of cohesionless soils are affected by a number of factors:

(1) Grain Size Distribution and Soil Types

The type of soil most susceptible to liquefaction is one in which the resistance to deformation is mobilized by friction between particles. If other factors such as grain shape, uniformity coefficient and relative density are equal, the frictional resistance of cohesionless soil decreases as the grain size of soils becomes smaller. Tsuchida (1970) summarized the results of sieve analyses performed on a number of alluvial and diluvial soils that were known to have liquefied or not to have liquefied during earthquakes. He proposed ranges of grain size curves separating liquefiable and nonliquefiable soils as shown in Fig. 3.13. The area within the two inner curves in the figure represents sands and silty sands, the soils with the lowest resistance to liquefaction. A soil with a gradation curve falling in the zones between the outer and inner curves is less likely to liquefy. Soils with a higher percentage of gravels tend to mobilize higher strength during shearing, and to dissipate excess pore pressures more rapidly than sands. However, there are case histories indicating that liquefaction has occurred in loose gravelly soils (Seed 1968; Ishihara 1985; Andrus et al. 1991) during severe ground shaking or when the gravel layer is confined by an impervious layer. The space between the two curves farthest to the left reflects the influence of fines in decreasing the tendency of sands to densify during seismic shearing. Fines with cohesion and cementation tend to make sand particles more difficult to liquefy or to seek denser arrangements. However, nonplastic fines such as rock flour, silt and tailing slimes may not have as much of this restraining effect. Ishihara (1985) stated that clay- or silt-size materials having a low plasticity index value will exhibit physical characteristics resembling those of cohesionless soils, and thus have a high degree of potential for liquefaction. Walker and Steward (1989), based on their extensive dynamic tests on silts, have also concluded that nonplastic and low plasticity silts, despite having their grain size distribution curves

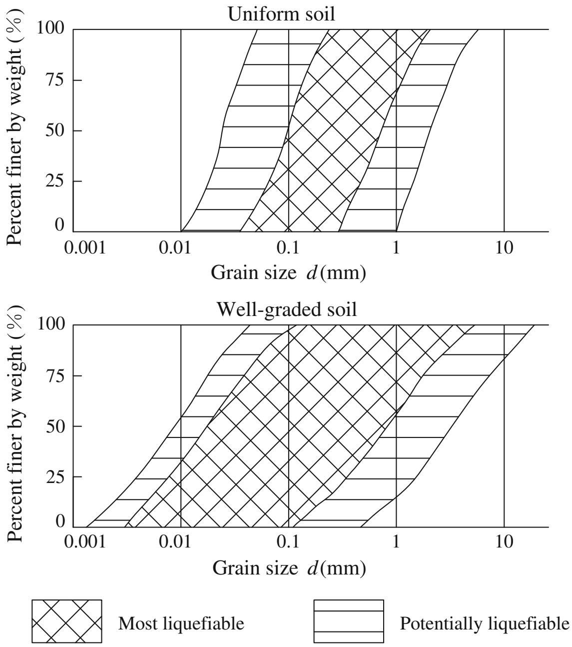

Fig. 3.13 Limits in the gradation curves separating liquefiable and nonliquefiable soils (Tsuchida 1970)

outside of Tsuchida's boundaries for soils susceptible to liquefaction, have a potential for liquefaction similar to that of sands and that increased plasticity will reduce the level of pore pressure response in silts. This reduction, however, is not significant enough to resist liquefaction for soils with plasticity indices of 5 or less.

Even though major slide movements during earthquakes have occurred in clay deposits, they are commonly considered to be nonliquefiable during earthquakes in the sense that an extensive zone of clay soil is converted into a heavy fluid condition. However, it is believed that quick clays may lose most of their strength after strong shaking and that other types of clay may lose a proportion of their strength resulting in slope failures. Frequently, landslides in clay deposits containing sand or silt lenses are initially triggered by the liquefaction of these lenses before any significant strength loss occurs in the clay. This has been supported by laboratory test results which indicate that the strain required to liquefy sands is considerably smaller than the strain required to overcome the peak strength of cohesive soils (Seed 1968; Poulos et al. 1985). There is also ample evidence to show that uniformly graded materials, generally having a uniformity coefficient smaller than five, are more susceptible to liquefaction than well-graded materials (Ross et al. 1969; Lee and Fitton 1969) and that for uniformly graded soils, fine sands tend to liquefy more easily than coarse sands, gravelly soils, silts, or clay.

(2) Relative Density

Laboratory test results and field case histories indicate that, for a given soil, initial void ratio or relative density is one of the most important factors controlling liquefaction. Liquefaction occurs principally in saturated clean sands and silty sands

Table 3.2 The relative density index D_r for possibility in liquefaction

Seismic fortification intensity	6	7	8	9
D_r	0.65	0.70	0.75	0.80–0.85

having a relative density less than 50 %. For dense sands, however, their tendency to dilate during cyclic shearing will generate negative pore-water pressures and increase their resistance to shear stress. The lower limit of relative density beyond which liquefaction will not occur is about 75 %. According to *Code for Hydropower Engineering Geological Investigation (GB50287-2006)*, it is specific that when the relative density D_r is smaller than values in Table 3.2, liquefaction probably happens during earthquake. During the Niigata earthquake of 1964 in Japan, in 7-M areas, liquefaction mostly occurred in the places with $D_r \leq 0.5$; and the sections with $D_r \geq 0.5$ can hardly be seen the liquefaction damage.

(3) Earthquake Loading Characteristics

The vulnerability of any cohesionless soil to liquefaction during an earthquake depends on the magnitude and number of cycles of stresses or strains induced in it by the earthquake shaking.

These in turn are related to the intensity, predominant frequency, and duration of ground shaking. The earthquake load is characterized in terms of the maximum acceleration. Generally when the surface maximum acceleration reaches $0.1g$ (g is the gravity acceleration, $1g = 980$ cm/s^2), liquefaction is potential to happen. Both field monitoring and experimental data indicate that liquefaction of soil under dynamic loading is related with the vibration frequency and duration. Such as the Alaska earthquake, most liquefaction occurred 90 s later after the earthquake happened. If that earthquake lasted only 45 s, it was probably that liquefaction hardly arose.

(4) Vertical Effective Stress and Overconsolidation

It is well known that an increase in the effective vertical stress increases the bearing capacity and shear strength of soil, and thereby increases the shear stress required to cause liquefaction and decreases the potential for liquefaction. From field observations it has been concluded by a number of investigators that saturated sands located deeper than 15–18 m are not likely to liquefy. These depths are in general agreement with Kishida (1969) who states that a saturated sandy soil is not liquefiable if the value of the effective overburden pressure exceeds 190 kN/m^2.

Both theory and experimental data show that for a given soil a higher overconsolidation ratio leads to higher lateral earth pressure at rest and thereby increases the shear stress ratio required to cause liquefaction. During the Xingtai Earthquake in China, there was a village in the same buried sand layer condition with other areas. Liquefaction did not happen here due to the difference with 2–3 m fill soil above. During the Niigata Earthquake in Japan, the areas with 2.75 m filling soils were all stable without liquefaction, while in other area severe liquefaction happened.

(5) Age and Origin of the Soils

Natural deposits of alluvial and fluvial origins generally have soil grains in the state of loose packing. These deposits are young, weak, and free from added strength due to cementation and aging. Youd and Hoose (1977) stated that, as a rule of thumb, alluvial deposits older than late Pleistocene (10,000–130,000 years) are unlikely to liquify except under severe earthquake loading conditions, while late Holocene deposits (1,000 years or less) are most likely to liquefy, and earlier Holocene (1,000–10,000 years) deposits are moderately liquefiable.

(6) Seismic Strain History

It has been demonstrated from laboratory test results that prior seismic strain history can significantly affect the resistance of soils to liquefaction (Finn et al. 1970; Seed et al. 1977; Singh et al. 1980). Low levels of prior seismic strain history, as a result of a series of previous shakings producing low levels of excess pore pressure, can significantly increase soil resistance to pore pressure buildup during subsequent cyclic loading. This increased resistance may result from uniform densification of the soil or from better interlocking of the particles in the original structure due to elimination of small local instabilities at the contact points without any general structural rearrangement taking place. Large strains, however, associated with large pore pressure generation and conditions of full liquefaction can develop weak zones in the soil due to uneven densification and redistribution of water content (National Research Council 1985; Whitman 1985), and thus lower the resistance of the soil to pore pressure generation during subsequent cyclic loading.

(7) Degree of Saturation

Liquefaction will not occur in dry soils. Only settlement, as a result of densification during shaking, may be of some concern. Very little is known on the liquefaction potential of partially saturated sands. Available laboratory test results (Sherif et al. 1977) show liquefaction resistance for soils increases with decreasing degree of saturation, and that sand samples with low degree of saturation can become liquefied only under severe and long duration of earthquake shaking.

(8) Thickness of Sand Layer

In order to induce extensive damage at level ground surface from liquefaction, the liquefied soil layer must be thick enough so that the resulting uplift pressure and amount of water expelled from the liquefied layer can result in ground rupture such as sand boiling and fissuring (Ishihara 1985; Dobry 1989). If the liquefied sand layer is thin and buried within a soil profile, the presence of a nonliquefiable surface layer may prevent the effects of the at-depth liquefaction from reaching the surface. Ishihara (1985) has set up a criterion to stipulate a threshold value for the thickness of a nonliquefiable surface layer to avoid ground damage due to liquefaction, as shown in Fig. 3.10. Although this figure is believed to be speculative and should not be used for design purposes, it provides initial guidance in this matter for sites having a buried liquefiable sand layer with a standard penetration resistance of less than 10 blows per 0.3 m. It should also be noted that even though the thickness of a nonliquefiable surface layer exceeds the threshold thickness shown in the figure, the ground surface may still experience some settlement which may be undesirable for certain settlement-sensitive structures. Like all of the empirical curves shown in this report, this figure, based on just three case histories, may need to be modified as more data become available.

3.5.3 Evaluation of Liquefaction Potential

To date, after 30 years of intensive research on this subject, much progress has been made in understanding the liquefaction phenomena of cohesionless soils under seismic loading. A variety of methods for evaluating the liquefaction potential of soils have been proposed. As mentioned above, the factors affecting sands or silts are various. Various procedures for evaluating the liquefaction potential of saturated soil deposits have been proposed in the past 20 years. These procedures, requiring various degrees of laboratory and/or in situ testing, may be classified into two categories: first aspect is empirical correlations between in situ characteristics and observed performance. Soil liquefaction characteristics determined by field performance have been correlated with a variety of soil parameters such as Standard Penetration Test (SPT) Resistance, Cone Penetration Resistance, Shear Wave Velocity and Resistivity and Capacitance of Soil. Second is threshold shear strain concept compared with the laboratory testing value. There exists for a given cohesionless soil a threshold shear strain, typically 0.01 %. If the peak shear strain induced by an earthquake does not exceed this strain, the shaking will not cause a buildup of excess pore pressure regardless of the number of loading cycles, and, therefore, liquefaction cannot occur. For the laboratory condition limitation for undisturbed saturated sands or silts, the former method is more applicable in practical engineering. And it has been adopted into relevant specific code. And during the in situ testing soil parameters, Standard Penetration Test (SPT) Resistance is used widely in many countries, such as China, Japan, and the United States.

The determination of vibrated liquefaction of soil may be carried out in two stages: preliminary determination and redetermination. During preliminary determination, soil stratum, which will not be excluded; and for soil stratum, which is likely to be liquefied according to preliminary determination, redetermination shall be performed to determine the liquefaction potential.

1. According to the experience, the preliminary determination can be carried out as follows:

(1) If a stratum belongs to the age of Quaternary late Pleistocene (Q_3) or earlier, it may be determined as nonliquefied soils for intensity 7–9.

(2) If the percentage of grain content with particle size bigger than 5 mm is equivalent to or larger than 70 %, it may be determined to be nonliquefaction. If the percentage of grain content with particle size larger than 5 mm is smaller than 70 %, and no other integral discriminative method is available for use, its liquefaction performance may be determined according to the portion of grain with particle size smaller than 5 mm. For soil with particle size smaller than 5 mm, if the

mass percentage of grain content is larger than 30 %, and the mass percentage of grain contents with particle size smaller than 0.005 mm, corresponding to aseismatic fortification intensity VII, VIII and IX, are not smaller than 10, 13 and 16 % respectively, it may be determined as nonliquefaction.

Note: The clay particles contain shall be determined by use of sodium heametaphosphate as the dispersant. When other methods are be used, it shall be correspond conversed according to relative provisions.

(3) For buildings with natural subsoil, the consequences of liquefaction need not be considered when the thickness of the overlying nonliquefied soils and the elevation of groundwater table comply with one of following conditions:

$$d_u > d_0 + d_b - 2$$
$$d_w > d_0 + d_b - 3$$
$$d_u + d_w > 1.5d_0 + 2d_b - 4.5$$

where d_w is the elevation of groundwater table (in m), for which the mean annual highest elevation during the reference period should be used, or the annual highest elevation in recent years may also be used; d_u is the thickness of the overlying nonliquefiable layer (in m), in which the thickness of mud and silt seams should be deduced; d_b is the foundation depth (in m), when it is less than 2 m, shall equal 2 m; d_0 is the reference depth of liquefaction soil (in m), it may be taken as the values presented in Fig. 3.14 (according to the earthquake disaster survey data some criteria are drawn in Fig. 3.14 including some safety factors).

2. When the sequence discriminated liquefaction need be considered base on the primary discrimination, the standard penetration tests shall be performed, in which the discriminated depth shall be taken as 15 m underground, but shall be taken as

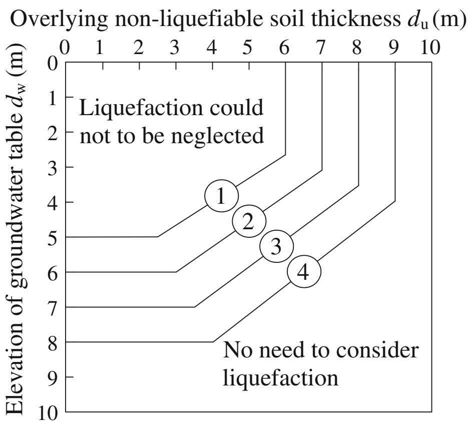

Curve	Intensity	
	Sand	Silt
1		7
2	7	8
3	8	9
4	9	

Fig. 3.14 The preliminary discrimination criteria for liquefaction according to two thicknesses (from Handbook of design and construction of underground engineering 1999)

20 m underground for the pile foundation or for the foundation buried depth greater than 5 m.

When the measured value of standard penetration resistance (in blow-number, and bar-length-modification is not included) is less than the critical value of that, the saturated soil shall be discriminated as liquefied soil; and other methods, if already proved successful, may also be used.

Within the depth of 15 m underground, the critical value of standard penetration resistance (in blow-number) for liquefaction discrimination may be calculated according to the following equation:

$$N_{cr} = N_0 \beta [\ln(0.6 d_s + 1.5) - 0.1 d_w] \sqrt{\frac{3}{\rho_c}} \tag{3.10}$$

Within the depth of 15–20 m underground, the critical value of standard penetration resistance (in blow-number) for liquefaction discrimination may be calculated according to the following equation:

$$N_{cr} = N_0 [2.4 - 0.1 d_w] \sqrt{\frac{3}{\rho_c}} \tag{3.11}$$

where N_{cr} is the critical value of standard penetration resistance (in blow-number) for liquefaction faction discrimination; N_0 is the reference value of standard penetration resistance (in blow-number) for liquefaction discrimination, it shall be taken from Table 3.3; d_s is the depth of standard penetration resistance for saturated soil (in m); ρ_c is the percentage of clay particle content; when it is less than 3 % or when the soil is sand, the value shall equal 3 %.

3. For the subsoil with liquefied soil layers, the level and thickness of soil layer shall be explored and the liquefaction index shall be calculated by the following equations, and then the liquefaction grades shall be comprehensively classified according to Table 3.4.

$$I_{le} = \sum_{i=1}^{n} \left(1 - \frac{N_i}{N_{cri}}\right) d_i w_i \tag{3.12}$$

Table 3.3 Reference value of standard penetration resistance

Design seismic group	Aseismatic fortification intensity		
	7	8	9
Group 1st	6 (8)	10 (13)	16
Group 2nd or 3rd	8 (10)	12 (15)	18

Note Values in the brackets are used for the design basic acceleration of ground motion is 0.15*g* and 0.30*g*

Table 3.4 Grade of liquefaction

Grade of liquefaction	Light	Moderate	Serious
Liquefaction index for discrimination depth is 15 m	$0 < I_{le} \leq 5$	$5 < I_{le} \leq 15$	$I_{le} > 15$
Liquefaction index for discrimination depth is 20 m	$0 < I_{le} \leq 6$	$6 < I_{le} \leq 18$	$I_{le} > 18$

where I_{le} is the liquefaction index: $I_{le} = \sum_{i=1}^{n} \left(1 - \frac{N_i}{N_{cri}}\right) d_i w_i n$; n is the total number of standard penetration test point in each bore within the discriminated depth under the ground surface; N_i, N_{cri} are measured value and critical value of standard penetration resistance (in blow-number) at ith point respectively, when the measured value is greater than the critical value, shall take as equal critical value; d_i is the thickness of soil layer (in m) at ith point, it may be taken as half of the difference in depth between the upper and lower neighboring standard penetration test points, but the upper point level shall not be less than elevation of groundwater table, and the lower point level not greater than the liquefaction depth; w_i is the weighted function value of the ith soil layer (in m^{-1}), which is considered the effect of the layer portion and level of the unit soil layer thickness. For discrimination depth is 15 m underground, such value is equal 10 when the depth of the midpoint of the layer is less than 5 m, is zero when it equals 15 m, and linear interpolation when it is between 5 and 15 m. For discrimination depth is 20 m underground, such value is equal 10 when the depth of the midpoint of the layer is less than 5 m, is zero when it equals 20 m, and linear interpolation when it is between 5 and 20 m.

4. Moreover, another method is recommended in *Code for Investigation of Geotechnical Engineering (GB50021-2001)* by Cone penetration tests to discriminate sand liquefaction. It was proposed by Ministry of Railway Institute of Science and Technology, and also suggested in international professional conference. This method is mainly based on the 125 series of testing information in different intensity area during Tangshan Earthquake. It is suitable for saturated sands and silts. The criterion is that, when the calculated specific penetration resistance or tip resistance is smaller than the critical specific penetration resistance or tip resistance, it is regarded as liquefaction.

A critical specific penetration resistance to discriminate the liquefaction of saturated sands was carried out as Eq. (3.13).

$$\begin{gathered} p_{scr} = p_{s0}\alpha_w\alpha_u\alpha_p \\ q_{ccr} = q_{c0}\alpha_w\alpha_u\alpha_p \\ \alpha_w = 1 - 0.065(d_w - 2) \\ \alpha_u = 1 - 0.05(d_u - 2) \end{gathered} \tag{3.13}$$

where p_{scr}, q_{ccr} is the critical specific penetration resistance or tip resistance of saturated sands, MPa; p_{s0}, q_{c0} is the base value of specific penetration resistance or tip resistance under conditions of 2 m groundwater table ($d_w = 2$ m) and 2 m overlying nonliquefiable soil ($d_u = 2$ m) (shown as Table 3.5); α_w is the groundwater table correction coefficient, it can be 1.13 when there is water and always has

Table 3.5 The base value of p_{s0}, q_{c0}

Aseismatic fortification intensity	7	8	9
p_{s0}(MPa)	5.0–6.0	11.5–13.0	18.0–20.0
q_{c0}(MPa)	4.6–5.5	10.5–11.8	16.4–18.2

Table 3.6 The correction coefficient of soil properties

Soil type	Sands	Silt	
Friction resistance ratio R_f	$R_f \leq 0.4$	$0.4 < R_f \leq 0.9$	$R_f > 0.9$
α_p	1.00	0.60	0.45

hydraulic connection all over a year; α_u is the correction coefficient of overlying nonliquefiable soil thickness, it can be 1.0 for deep foundation pit; d_w is the buried depth of groundwater table; d_u is the overlying nonliquefiable soil thickness, m; α_p is the correction coefficient of cone penetration friction resistance ratio, shown as Table 3.6.

One more method is the shear wave velocity discrimination for liquefaction according to the *Code for Investigation of Geotechnical Engineering (GB50021-2001)*.

When the shear wave velocity of soil stratum is larger than the upper limit one calculated by Eq. (3.14) or Eq. (3.15), it may be determined as nonliquefaction.

Sand:

$$v_{scr} = \sqrt{K_c\left(d_s + 0.01d_s^2\right)} \tag{3.14}$$

Silt:

$$v_{scr} = \sqrt{K_c\left(d_s - 0.0133d_s^2\right)} \tag{3.15}$$

where v_{scr} is the critical value of shear wave velocity of saturated sand or silt, m/s; K_c is the empirical coefficient, it is 92, 130, 184 in saturated sands and 42, 60 and 84 in saturated silts for intensity 7, 8, and 9 respectively; d_s is the depth of measuring point for shear wave velocity in sand or silt, m.

According to the specific code, any single method results should comprehensively analyzed with other method when the discrimination could not be determined easily.

There is another method called maximum pore-water pressure discrimination, proposed by the Institute of Science in water resource and hydropower of China in the Fifth International Conference on soil mechanics and foundation engineering. A relevant paper conducted the research on liquefaction analysis on sand foundation and sandy slope. This paper suggested that the triaxial testing apparatus on shaking table (vertical vibration) can be used for liquefaction study in the

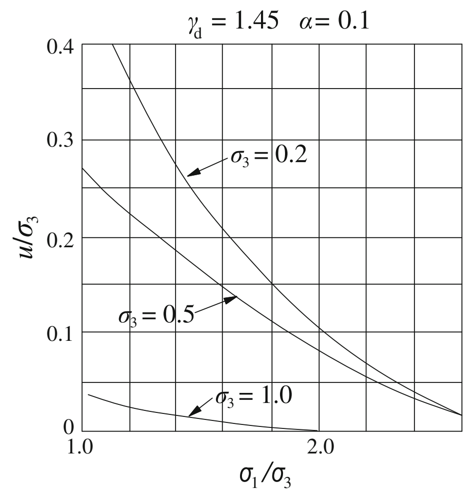

Fig. 3.15 The pore-water pressure under different stress conditions

laboratory. Maximum and minimum principal stresses σ_1 and σ_3 were applied as confining pressure and vertical pressure in the triaxial test on the shaking table. The vertical pressure were employed to vibrate during $\sigma_1 \pm \Delta\sigma_1$, where $\Delta\sigma_1 = \sigma_1 \frac{\alpha}{g}$, α was the vibration acceleration. The maximum pore-water pressure u (undrained) was measured during the loading of σ_3 and $\sigma_1 \pm \Delta\sigma_1$. By virtue of this, the dynamic stability of sand foundation can be checking based on the method in soil mechanics.

Figure 3.15 is the maximum pore-water pressure field measured data under different dynamic loading in a muddy fine sands (D_{50} = 0.06 mm, coefficient of uniformity $\mu_u = 1.4$). From the figure, the smaller the confining pressure σ_3 is, the maximum pore-water pressure generated is larger. u/σ_3 increased as the stress ratio σ_1/σ_3 declined.

5. Simplified stress comparison method

Basically, this method is to compare the shear stress generated during vibration loading to the critical shear stress inducing liquefaction (i.e., the shear strength under a certain dynamic loading) and hereby to discriminate the range of liquefaction. For this purpose, several problems should be figured out. First the shear stress values in different depths under the vibration loading, by practical experience or theoretical computation. Second the critical shear stress for liquefaction under different stress conditions, analyzing in situ for liquefied area and nonliquefied area, or through laboratory tests, such as dynamic triaxial tests and reciprocated simple shear tests. These two aspects are much complicated. Here a simplified method proposed by Seed is introduced.

(1) The simplified calculation for the shear stress generated during earthquakes:

$$\tau_{av} \approx 0.65 \frac{\gamma h}{g} \alpha_{max} \cdot \gamma_d \tag{3.16}$$

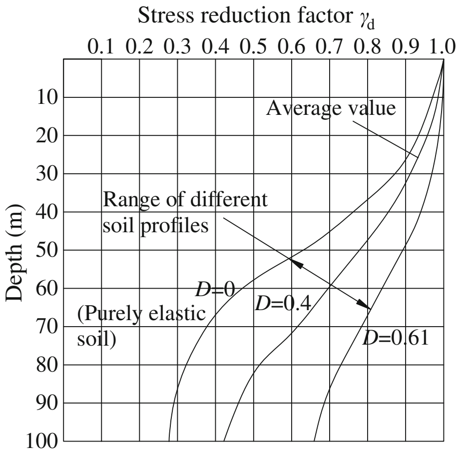

Fig. 3.16 Stress reduction factor in relation to depth (Seed and Idriss 1971)

where τ_{av} is the average peak shear stress; γ is the unit weight of the soils above the studying depth; h is the buried depth of purpose soils; α_{max} is the maximum horizontal ground acceleration during earthquakes; γ_d is the reduction factor of dynamic stress, whose value is smaller than 1, depending on the soil type and buried depth shown as Fig. 3.16.

From the above figure, it can be seen that in the upper 9.00–12.00 m, the variation of γ_d marginally changed. The average value in the dash curve can be used.When in the depth of:

$$\begin{aligned} 3\,\mathrm{m},\ \gamma_d &= 0.98 \\ 6\,\mathrm{m},\ \gamma_d &= 0.95 \\ 9\,\mathrm{m},\ \gamma_d &= 0.92 \\ 12\,\mathrm{m},\ \gamma_d &= 0.85 \end{aligned}$$

Nevertheless the deviation brought in is generally less than 5 %. According to Eq. (3.16), if the maximum acceleration generated during the earthquake can be known, as well as unit weight of soil, then the average shear stress under different depth during the earthquake can be calculated.

(2) The simplified calculation for critical shear stress inducing liquefaction

The liquefied shear stress under reciprocated vibration loading can be determined by analyzing the stress condition of liquefaction during earthquakes. It can also be figured out by specific laboratory tests.

According to the previous research data, the relation of the liquefied shear stress ratio in situ and measured in the laboratory presented in Eq. (3.17).

$$\left(\frac{\tau_d}{\sigma'_0}\right) = \left(\frac{\Delta\sigma_1}{2\sigma_3}\right)_{50} \cdot C_r \frac{D_r}{50} \tag{3.17}$$

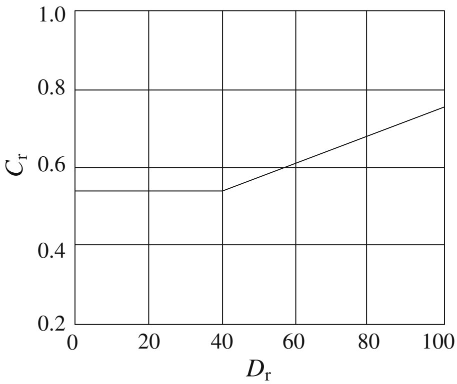

Fig. 3.17 The relation of modification factor with the relative density

where τ_d is the liquefied shear stress on the horizontal surface; σ'_0 is the initial stress; $\sigma_1 + \Delta\sigma_1$ is the vertical stress under cyclic loading; σ_3 is the initial consolidation stress, i.e., confining pressure. C_r is the modification factor from laboratory data to the in situ value, shown as Fig. 3.17; $\left(\frac{\Delta\sigma_1}{2\sigma_3}\right)_{50}$ is the liquefied stress ratio under triaxial tests. The relative density of the sand was controlled in 50 % during the tests.

Figure 3.19 was the result of the stress ratios under different particle size (represented by d_{50}) and the same relative density of 50 %. Even though these two curves obtained from two different researchers, the results were much consistent with each other. Hence we can use Fig. 3.18 to get the rough linear relationship between liquefied shear stress ratio and relative density of sand, combined with Eq. (3.15), $\left(\frac{\tau_d}{\sigma'_0}\right)$ can be calculated.

(3) Comparing the value calculated from Eq. (3.16) τ_{av} and Eq. (3.17) τ_d, the area of $\tau_d < \tau_{av}$ is the range of liquefaction, presented in Fig. 3.19.

6. The critical acceleration method

This method is based on the laboratory dynamic triaxial tests. During the tests, the sample was saturated and drained consolidation under confining pressure σ_3

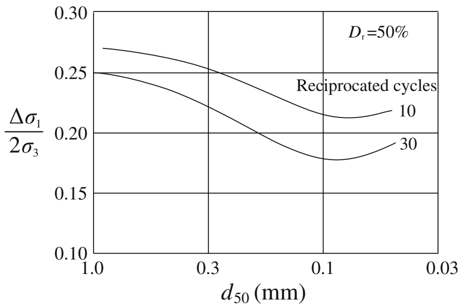

Fig. 3.18 The relation between shear stress ration and grain size

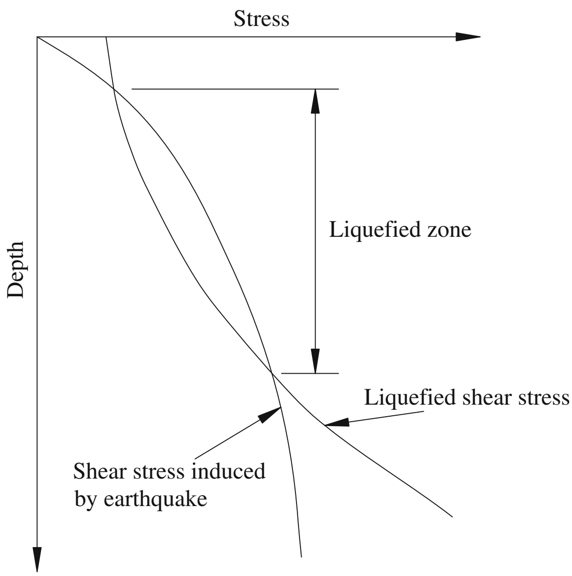

Fig. 3.19 The relation of liquefaction discrimination

was performed, then the drainage valves were closed for the undrained vibration loading. Gradually increasing the vibration acceleration, a critical acceleration to make sand liquefaction can be found under a certain confining pressure σ_3. Then the sand sample were remolded to measure the critical acceleration under different confining pressures. A relation of $\sigma_3 \sim a_c$ can be deduced out. In addition, the critical acceleration a_c under different σ_3, σ_1 can be figured out during the tests as well. Then the curve of $(\sigma_1 - \sigma_3) \sim a_c$ was acquired.

To discriminate the potential of liquefaction, it can be derived by calculation method or experimental method. The maximum and minimum primary stress of σ_3, σ_1 are both figured out in each calculation point of sand foundation under the designed loading; according to the $(\sigma_1 - \sigma_3) \sim a_c$ curve, the a_c value of each point can be determined. All the same a_c values are connected to draw isolines in each a_c value. During a practical earthquake, the acceleration is a'_c. All the areas of $a_c \leq a'_c$ are the potential liquefaction places.

The above six methods, except maximum pore-water pressure method and the critical acceleration method are time consuming and contain a lot of work based on laboratory dynamic triaxial tests, are really convenient and simply to be carried out.

3.5.4 Anti-Liquefaction Measurement

Numerous case histories on earthquake activities have documented that liquefaction of cohesionless soils is one of the major causes for structure damage and human casualties. However, one can ensure that liquefaction in loose cohesionless soils cannot be triggered if the effective stress of the soil during shaking is always greater than zero. The development of initial liquefaction in dense sands is often of no practical significance, since subsequent straining will decrease the amount of pore pressure generated. Hence, on one hand, if the potentially liquefiable soil layer is located at the ground surface and is not thicker than 3.5 m, the most economical solution may be removal and replacement with properly compacted nonliquefiable soils. However, for liquefaction-prone soil layers located deeper than 3.5 m from the ground surface, ground reinforcement techniques such as dynamic compaction, vibroflotation, stone columns and grouting may be the optimal solution. Or using of piling to bypass the potentially liquefiable zones. This is the brute force and cost-expensive solution. Piling would need to be designed for the unsupported length equivalent to the liquefied depth and for potential negative skin friction from clay layers overlying liquefiable zones. On the other hand, from the view of superstructure without soil improvements, increasing the overall stiffness and balance-symmetric ability in the superstructure (avoiding to employ differential settlement-sensitive structure) or strengthening the integrity and rigidity of the foundation (such as raft foundation, box foundation, or cross-strip foundation) can effectively improve the ability of balancing the differential settlement in buildings and then mitigate the consequences of foundation liquefaction damage.

From the investigation of earthquake disasters, the circumstances differed a lot whether the liquefied layers located directly underlying the foundation or interbedded by a nonliquefied layer. The consequences of latter were mitigated greatly. Therefore, if there is a nonliquefied layer close to the ground surface; and the building upper loads are not so large, shallow foundation should be applied to best utilize this nonliquefiable layer as the bearing layer. Similarly, raising the ground surface elevation to increase the overlying pressure by filling soil is also an effective measurement.

In total, a rational anti-liquefaction measure is really important, in which safety and cost should be both cared. Comprehensively considering the foundation liquefaction grade and the specific superstructure configuration, the option can be determined by the seismic code or previous practical experience.

3.6 Pore-Water Pressure Problems

3.6.1 The Influence of Pore-Water Pressure on Shear Strength

In an undrained triaxial test on a saturated foundation clay, each increase of the cell pressure will lead to increase of the pore-water pressure. According to effective stress theory and Skempton’s formula, this can be described in Eq. (3.18).

$$\begin{cases} \sigma = \sigma' + u \\ \Delta u = B[\Delta\sigma_3 + A(\Delta\sigma_1 - \Delta\sigma_3)] \end{cases} \tag{3.18}$$

where σ is the total stress, kPa; σ' is the effective stress, kPa; $\Delta\sigma_1$, $\Delta\sigma_3$ are the maximum and minimum primary stress increment, respectively, kPa; A, B are coefficients of pore-water pressure called as Skempton's coefficients: B is related to the saturation of soil, in which complete saturation refers to B = 1; complete dry condition B = 0. The values of B observed in tests are usually somewhat smaller than 1. A is related to the stress history of soils. Higher overconsolidation ratio results in smaller A value. The coefficient A various values, usually between 0 and 0.5 are found, but sometimes even negative values have been obtained.

Hence, when changes occur, positive or negative pore-water pressure can either be generated. Since the effective stress on the soil particle skeleton, equals to the difference between the total pore-water pressure and pore-water pressure, the undrained pore-water pressure variation only affects the effective normal stress applied on the soil skeleton, while has no influence on the shear stress.

$$\tau = \frac{\sigma'_1 - \sigma'_3}{2}\sin 2\alpha = \frac{(\sigma_1 - u) - (\sigma_3 - u)}{2}\sin 2\alpha = \frac{\sigma_1 - \sigma_3}{2}\sin 2\alpha \tag{3.19}$$

Under a certain total stress condition, the positive pore-water pressure will weaken the shear strength of soils. From Fig. 3.20, if the initial stress condition is represented by the Mohr circle A, and a positive pore-water pressure is generated during the undrained triaxial test, resulting the left movement in the Mohr circles and closer to the strength envelop. When the Mohr circle is tangent to the strength envelop curve, such as B, the soil strength failure happens. On the contrary if the negative pore-water pressure is generated the Mohr circle moves to right and results in safer circumstance. In practical engineering, acknowledge of the variation of pore-water pressure can really make great sense.

Fig. 3.20 The influence of pore-water pressure on shear strength

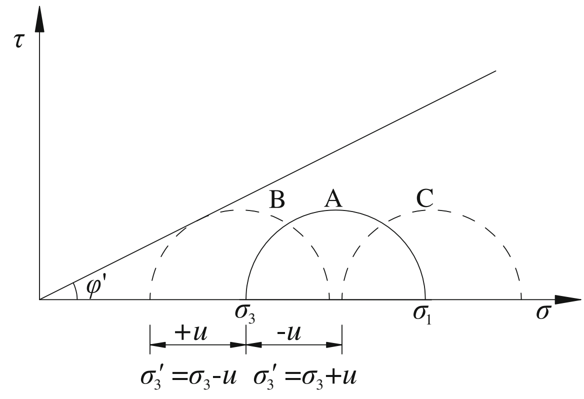

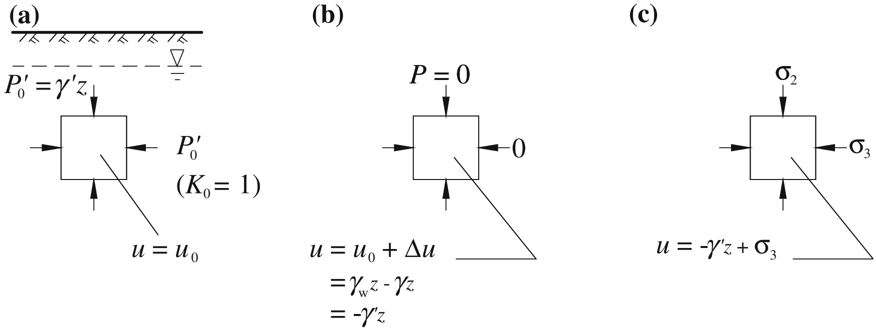

Fig. 3.21 The undrained stress variation during sampling. **a** In-situ condition. **b** After sampling. **c** Tri-axial testing

Figure 3.21 presents an example of undrained stress variation process during sampling. In Fig. 3.21a shows the undisturbed stress condition in situ. Assuming the coefficient of the lateral pressure at rest $K_0 = 1$, the field consolidation pressure is $P_0' = \gamma' \cdot z$; and the initial pore-water pressure is $u_0 = \gamma_w \cdot z$; total stress is $P = \gamma \cdot z$. If the sampling technology is advanced enough to hardly bring disturbance for the soil, the stresses originally applied on the sample are all released. The variation of total stress is $-P = -\gamma \cdot z$. It transfers into pore-water pressure $\Delta u = -\gamma \cdot z$ under undrained condition. Then the whole pore-water pressure is $u = u_0 + \Delta u = \gamma_w \cdot z - \gamma \cdot z = -\gamma' \cdot z$, resulting the effective stress on the soil particle skeleton as:

$$\sigma' = \sigma - u = 0 - (-\gamma' \cdot z) = \gamma' \cdot z = P_0'$$

This calculation indicates that, the stress is released after soil sampling, but the effective stress on soil particle skeleton has not changed. Figure 3.21b, c present the stress conditions deploying in laboratory triaxial tests.

The above analysis makes significant sense on the excavation engineering. The excavation can be considered as a negative load, which will result in decreasing total stresses, and therefore decreasing pore pressures immediately after the excavation. Due to consolidation, however, the pore-water pressures later will gradually increase, and they will ultimately be reduced to their original value, as determined by the hydrologic conditions. Thus the effective stresses will be reduced in the consolidation process, so that the shear strength of the soil is reduced. This means that in the course of time the risk of a sliding failure may increase. A trench may be stable for a short time, especially because of the increased strength due to the negative pore pressures created by the excavation, so during the excavation construction, the soil in the bottom of foundation pit should be protected as soon as possible and lay the cushion and pour the lining plate in short time.

3.6.2 Instantaneous and Long-Term Stability in Foundation Pit in Saturated Clay

During the stability analysis in foundation pit excavation, the shear strength of soil should be considered under the influences of loading mode and time. Analyzing the relative variation of stress and strength is the first step in the stability study and also the most important part. By virtue of this, all variety of stages in the whole foundation pit project can be under well consideration and control.

Figure 3.22 shows an embankment project in the saturated soft clay foundation. The stress condition of point a is fully depicted in Fig. 3.23a, b. The shear stress increases with the filling load rising. It approaches the highest at the onset of completion. And the initial pore-water pressure equals to the static pore-water pressure $\gamma_w \cdot h_0$. Due to the poor permeability, undrained condition can be logically assumed, i.e., the excess pore-water pressure could not dissipate during the filling load and the pore-water pressure ramps as the filling height rises. Shown as Fig. 3.23b, the coefficient A of pore-water pressure is arbitrary and pore-water pressure always positive value only otherwise large negative A exists. On the completion of embankment, the shear strength is consistent with the undrained shear strength at the beginning of construction (Fig. 3.23c).

After the completion of soil filling in embankment, i.e., at the time of t_1, the total stress keeps in a constant but the excess pore-water pressure dissipates gradually and reach zero at the full consolidated time of t_2. Consolidation makes the pore-water pressure decline, void ratio decrease and effective stress and shear strength augment both. Provided pore-water pressure value, the shear strength at any time can be evaluated according to the effective stress indices c' and φ'. Hence, the stability analysis on the completion should utilize total stress and undrained strength methods. And the long-term stability should apply effective stress and effective indices analysis. From Fig. 3.23d can be easily seen that, after the completion of filling, the foundation gets through a most adverse circumstance. Over this stage, the safety degree is increasing with time.

Figure 3.24 presents the excavation in saturated soft clay. The stress condition of point a is shown as the figure (Fig. 3.25). Excavation releases the overlying pressure, resulting in decrease of pore-water pressure and occurrence of negative

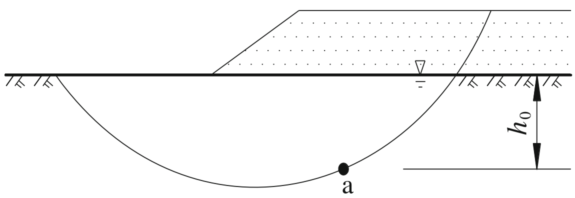

Fig. 3.22 The filling embankment on the soft foundation

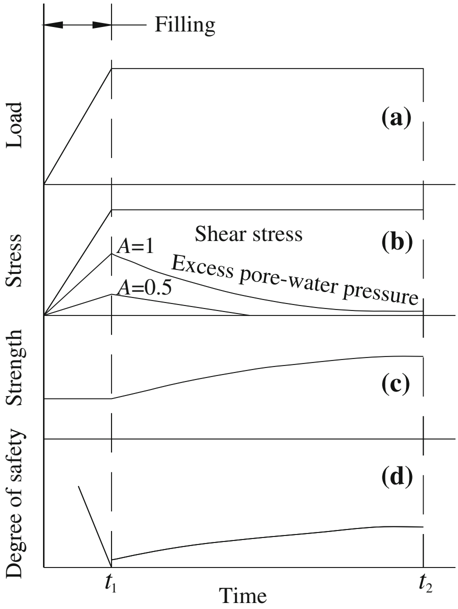

Fig. 3.23 The stability conditions during filling

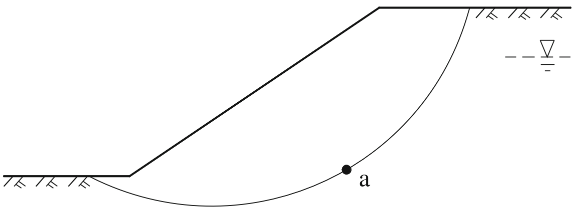

Fig. 3.24 The excavation on the soft foundation

pore-water pressure. If the pore-water pressure coefficient B equals to 1, the variation of pore-water pressure is following Eq. (3.20).

$$\Delta u = \Delta\sigma_3 + A(\Delta\sigma_1 - \Delta\sigma_3) \tag{3.20}$$

During the slope excavation, the minor primary stress declines more than the major primary stress. Hence the variation of the minor primary stress $\Delta\sigma_3$ is negative; the excess pore-water pressure Δu is negative at most circumstance. At the onset of completion of excavation, the shear strength of point a reaches the highest value; and because of the negative excess pore-water pressure, the shear strength is still equal to the initial shear strength before excavation. With the expansion of the soft clay after the excavation unloading, the negative pore-water pressure dissipates

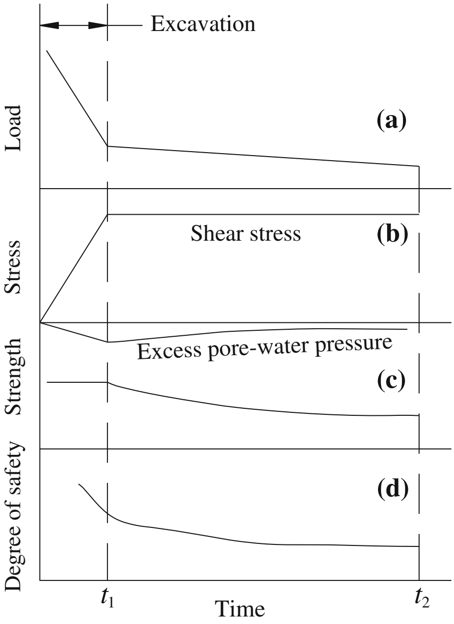

Fig. 3.25 The stability conditions of excavation **a** Load; **b** Stress; **c** Strength; **d** Degree of safety

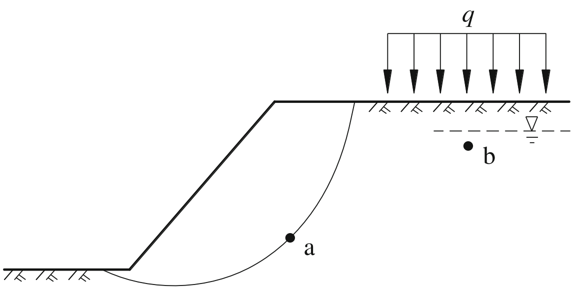

Fig. 3.26 Surcharge conditions

gradually; and the shear strength decreases accordingly. During a long-time duration, the negative pore-water pressure dissipates to zero resulting in lowest shear strength. Therefore, it is not hard to understand, excavation is opposite to filling circumstance. The stability after the completion is better than the long-term stability. The safety degree decreases with time.

Figure 3.26 shows the surcharge influence on foundation pit stability. The excess pore-water pressure induced by large-area surcharge on the slope top, such as heavy buildings or piling, etc., constructions, radiantly dissipates to drainage exit. The water flows from b to a, which increase the pore-water pressure at point a.

The stability conditions are depicted in Fig. 3.27. Assuming the surcharge load has some distance from the slope surface, the stress conditions is not conspicuously influenced on the circle sliding surface. And the shear stress keeps the same

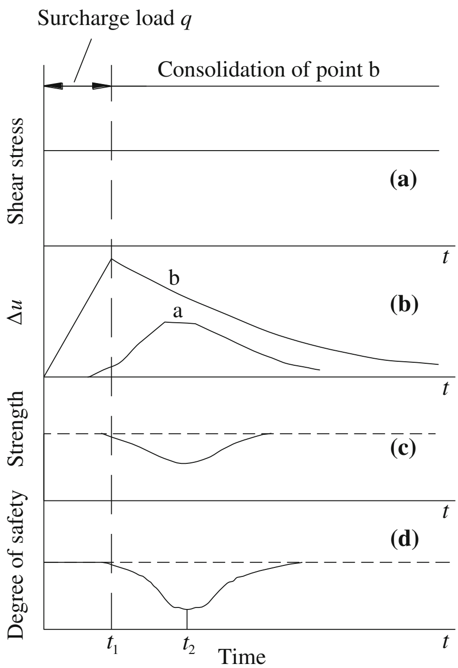

Fig. 3.27 The stability conditions under variable loading **a** Shear stress; **b** Δu; **c** Strength; **d** Degree of safety

(Fig. 3.27a). The pore-water pressure at point b increases by surcharge loading. As the water radiantly drains down away to the drainage exit, the excess pore-water pressure gradually ramps to highest value at point a. The augment of pore-water pressure makes the shear strength and safety degree both decreases at point a. It can be seen that, at a certain time t_2, the safety degree has a minimum value. In this circumstance, the potential dangerous is greatest. Hence, even if there are enough instantaneous stability and long-term stability, the slope is still has possibility to failure.

According to the above analysis, the stability of foundation pit is related to the loading mode, pore-water pressure, effective stress and soil strength. Some empirical experiences are summarized in Table 3.7 as reference.

3.7 Seepage

3.7.1 The Stability of Foundation Pit with Retaining Wall Under Seepage Condition

During the excavation in saturated soft clay, supporting structures need to be conducted. Sheet piles, underground diaphragm wall, cement mixing piles, or some other bored piles are usually utilized to seal the groundwater during construction.

Table 3.7 The measurements for improving the stability of foundation

Loading	Variation in stability	Measurement
Filling (loading)	Poorest stability on the completion of filling and then increase with time	Control the loading rate to have enough time for the dissipation of excess pore-water pressure; sand well can be used in foundation
Excavation (unloading)	Highest stability on the completion of excavation and then decrease with time	Protect the soil at pit bottom to avoid disturbance. Place cushions as soon as excavating to the design elevation
Large-area surcharge (overloading)	Most dangerous condition occurs after a certain duration after the completion of construction	Reasonably arrange surcharging area. Avoid piling, blasting activities nearby the slope top

Due to the high groundwater level, groundwater flow lines and equipotential lines are focused around the supporting structure, shown as Fig. 3.28. Hence the seepage failure can easily happen at the bottom of foundation pit. So the embedded depth should be designed appropriately to resist the seepage failure and enough safety degree for the seepage stability.

Figure 3.28 shows a foundation pit with supporting structure. The planar seepage calculation is shown as Fig. 3.29. 3-3'and 7-7' are assumed to be the water level equipotential lines, by which the foundation pit is divided into two parts I and II. Part I has the same seepage mode of the entrance and exit in foundation seepage calculation of gate dam. Part II is equivalent to the half part of $2S_2$ length flat floor seepage condition (Fig. 3.30). According to the fluid mechanics, the drag coefficients of these two conditions are presented in Fig. 3.31, in which, ξ_1 is the drag coefficient of Part I, determined by parameter $\frac{S_1}{T_1}$ and the $\frac{T_2}{b} = 0$ curve; ξ_2 is the drag coefficient of Part II, determined by parameters $\frac{S_2}{T_2}$ and $\frac{T_2}{b}$. Hereby the seepage capacity from one single side of sheet piles is:

$$q = Kh\frac{1}{\xi_1 + \xi_2} \tag{3.21}$$

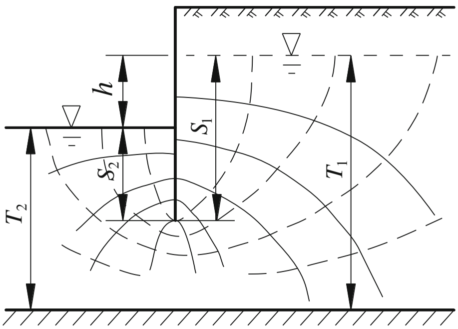

Fig. 3.28 Groundwater flow lines and equipotential lines

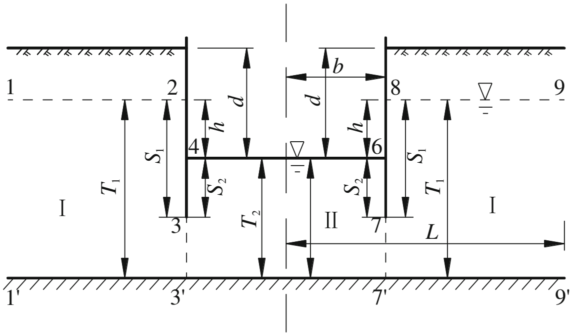

Fig. 3.29 Planar seepage calculation schematic

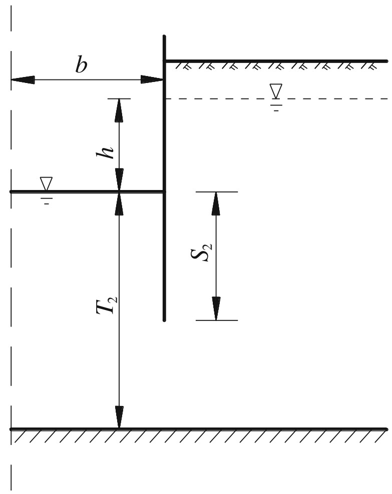

Fig. 3.30 Schematic in Part II (from Handbook of excavation engineering 1997)

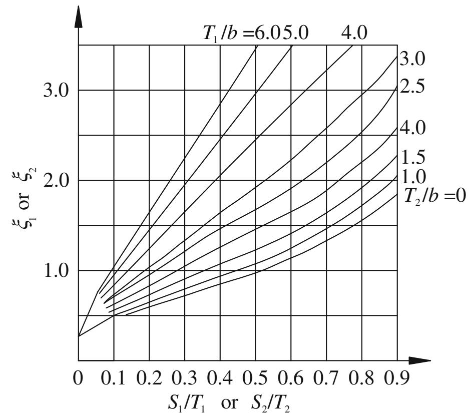

Fig. 3.31 Drag coefficients

The water head at the end of supporting structure of point 3 or 7 is:

$$h_{\mathrm{F}} = h\frac{\xi_2}{\xi_1 + \xi_2} \tag{3.22}$$

Then the hydraulic gradient of the exit of foundation pit bottom (point 3 or 7) is:

$$I_{\mathrm{F}} = \frac{h_{\mathrm{F}}}{S_2} \tag{3.23}$$

The critical hydraulic gradient for seepage stability is $I_c = 1 = I_F$; then the embedded depth of supporting structure should be:

$$S_2 \geq h_{\mathrm{F}} \tag{3.24}$$

For the three-dimensional seepage calculation, it can be modified by the planar calculation results.

For the circular foundation pit,

$$q = 0.8Kh\frac{1}{\xi_1 + \xi_2} \tag{3.25}$$

$$h_{\mathrm{F}} = 1.3h\frac{\xi_2}{\xi_1 + \xi_2} \tag{3.26}$$

where q is the seepage flux over unit length sheet pile, m^3/day. Thus the total seepage flux in circular foundation pit is $Q = 2\pi Rq$, where R is the radius of the foundation pit.

For square foundation pit,

$$q = 0.75Kh\frac{1}{\xi_1 + \xi_2} \tag{3.27}$$

$$h'_{\mathrm{F}} = 1.3h\frac{\xi_2}{\xi_1 + \xi_2} \tag{3.28}$$

$$h''_{\mathrm{F}} = 1.7h\frac{\xi_2}{\xi_1 + \xi_2} \tag{3.29}$$

where q is the seepage flux over unit length sheet pile, m^3/day. Thus the total seepage flux in circular foundation pit is $Q = 8lq$ (m^3/day), where l is the half length of the foundation pit side. h'_{F} and h''_{F} are the water head of center point and corner point of a foundation pit side, respectively.

Calculation value indicates the water head has highest value in the corner point. Thus the seepage instability can easily happen in the corner point. Hereby the embedded depth should be designed deeper in the corner than in the center positions.

As for the foundation pit in other geometries, such as triangular foundation pit, the water head in the corner point of short side can be calculated the same as square foundation pit, while for the head water in the center point of longer side, when the length–width ratio is close to or over 2, it can be calculated by planar seepage, without modification; As for polygon foundation pit, it can be equivalent to a circular foundation pit for the calculation.

3.7.2 The Stability of Slope Under Seepage Condition

During the excavation without well dewatering, seepage flow exists in the slope surface. The dynamic hydraulic action brings in adverse influence for the slope stability. Figure 3.32 describes the circumstance of seepage curve flowing through the slope surface. The groundwater flows downward to generate a hydrodynamic force, promoting the soil to slide down. The hydrodynamic force can be calculated by flow net analysis. In practice, it can be simply determined by mean hydraulic gradient.

In Fig. 3.32, point A and B are the intersection points of seepage line and sliding surface. Hence the mean hydraulic gradient is the slope of line AB. Hereby the total hydrodynamic force T of the sliding soil above the seepage line is:

$$T = \gamma_{\mathrm{w}} IA, \tag{3.30}$$

where γ_{w} is the water unit weight, kN/m^3; I is the horizontal hydraulic gradient over the applying area; H is the water head difference between point A and B, m; L is the horizontal distance between point A and B, m; A is the sliding area of the soil above the seepage line, m^2.

The seepage force T is conducted on the soil downward, resulting in a sliding moment of $T \cdot e$, where e is the distance of seepage force to the sliding center O. The point of action T can be assumed in the centroid of area A; and the direction is

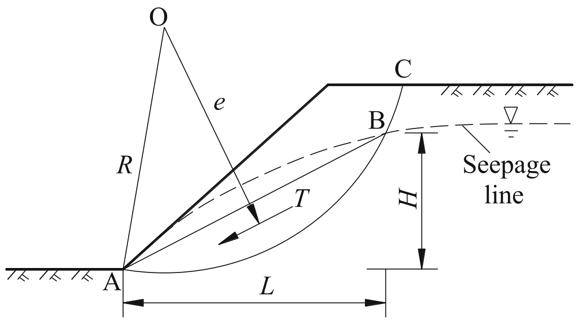

Fig. 3.32 The influence of seepage on stability

parallel to line AB. Thus the stability calculation formula can be modified as Eq. (3.31).

$$F_s = M_{\text{slide}-\text{resistant}} / (M_{\text{slide}} + Te) \tag{3.31}$$

where $M_{\text{slide-resistant}}$ is the slide-resistant moment; M_{slide} is the slide moment; Te is the seepage-slide moment.

3.8 Piping and Soil Displacement in Foundation Pit Bottom

The water exists between two stable aquitards bearing static water pressure is called the confined pressure water. It is formed closely related to the geological development and plays an important role in the underground environmental geological problems.

3.8.1 Piping in the Foundation Pit

When confined water layer exists under the foundation pit, excavation decreases the thickness of overlying aquitard to some extent; the water head of confined water may break or destroy the pit bottom and results in piping. There are several different piping behaviors as below:

(1) Cracking of pit bottom; mesh or branch fissures occur and water pouring out with fine particles.
(2) Quicksand in the pit bottom; slope instability and the entire foundation suspending flow.
(3) Boiling sands; water accumulates in the pit and disturbs the foundation.

Some conditions inducing the occurrence of piping in foundation pit during excavation are presented in Fig. 3.33. From the equilibrium condition of aquitard

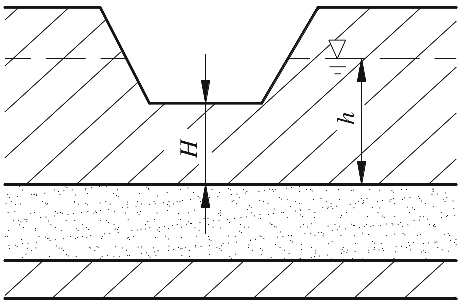

Fig. 3.33 The minimum aquitard thickness beneath the foundation pit

thickness beneath the pit bottom during excavation and the confined water pressure, there is some requirement on the minimum thickness H.

$$H = \frac{\gamma_w}{\gamma'} \cdot h \tag{3.32}$$

When

$$H > \frac{\gamma_w}{\gamma'} \cdot h \tag{3.33}$$

piping can hardly happen;

When

$$H < \frac{\gamma_w}{\gamma'} \cdot h \tag{3.34}$$

piping may happen, where H is the thickness of aquitard beneath the pit bottom after excavation, m; γ' is the effective (buoyant) unit weight of relevant soil, kN/m^3; γ_w is the unit weight of water, kN/m^3; h is the water head difference between confined water pressure and the elevation of aquitard baseline, m.

When $H < \frac{\gamma_w}{\gamma'} \cdot h$, measurement should be taken to avoid piping. Relief well is a good way to decrease the confined water head of the foundation pit bottom. During the dewatering process of relief well, the pore-water pressure in the soil should be monitored in real time. Shown as Fig. 3.34, the pore-water pressure of point C at the roof of the confined aquifer should be smaller than 70 % of the total stress. When the excavation surface is very narrow, this condition can be marginally flexible, since the shear strength of soil has some resistance to the bottom heave.

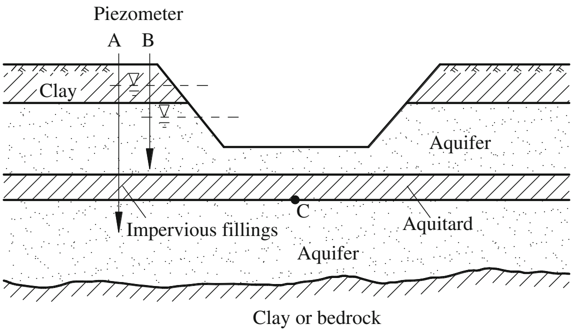

Fig. 3.34 The confined water pressure circumstance in foundation pit excavation

3.8.2 Soil Displacement

When the open caisson sinks close to the design depth, the thickness of the aquitard beneath is not large enough; it is probable cracked by the confined water pressure in the underlying sand layers (Fig. 3.35). The consequence is that large amount of sand boils rush into the caisson; the caisson sinks suddenly and substantial large-area ground subsidence occurs surrounding the caisson. When the caisson sinks undrained; and the water depth in the caisson is not enough; the plain concrete in the bottom is insufficient to balance the confined water pressure beneath; it can also induce the bottom floor of the caisson is cracked and punched by confined water pressure. The reason of the above problem is mainly contributed by the lack of enough borehole geological information. The engineering geological and hydrological conditions within the areas in 1.3 times of excavation depth are not well known before excavation. The stability of the finite-thickness aquitard overlying the confined water layer (Fig. 3.36) can be determined by following formula, by assuming the confined water head is stable at the elevation of ±0.00.

$$c \cdot u \cdot (mH) + F \cdot \gamma_s \cdot (mH) \geq F \cdot \gamma_w \cdot H_w$$

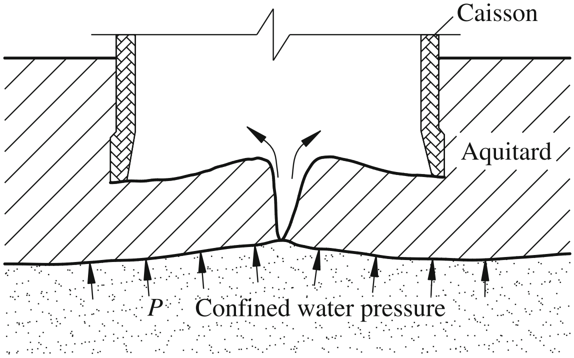

Fig. 3.35 The soil displacement induced by confined water pressure in the pit bottom

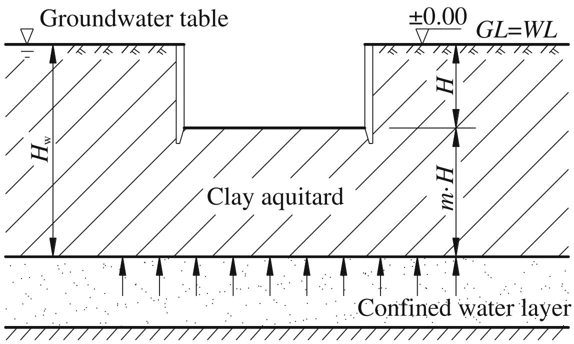

Fig. 3.36 The open caisson above a certain thickness of aquitard

Since the tension resistance of soil material is really poor, herein the cohesive effect c is ignored; the equilibrium condition can be simplified.

$$F \cdot \gamma_s \cdot (mH) \geq F \cdot \gamma_w \cdot H_w$$

$$\gamma_s \cdot (mH) \geq \gamma_w \cdot H_w$$

Because, $H_w = H + mH = H(1 + m)$,
thus

$$\gamma_s \cdot (mH) \geq \gamma_w \cdot H \cdot (1 + m) \tag{3.35}$$

From Eq. (3.35), we can get m by Eq. (3.36):

$$m \geq \frac{\gamma_w}{\gamma_s - \gamma_w} \tag{3.36}$$

where F is the bottom area of open caisson, m^2; γ_s' is the unit weight of the below aquitard layer, kN/m^3; u is the perimeter of inner wall of cutting edge, m; γ_w is the unit weight of water, kN/m^3; H_w is the confined water head of the underlying sand layer below the aquitard, m; H is the depth of the open caisson, m.

If $\gamma_w = 10\ \mathrm{kN/m^3}$, $\gamma_s = 18\ \mathrm{kN/m^3}$, the equilibrium condition could not be broken when Eq. (3.36) can be achieved.

$$m \geq \frac{10}{18 - 10} = 1.25$$

3.8.3 The Foundation Pit Bottom Stability Encountering Confined Water Pressure

If the thickness of the aquitard layer is not enough beneath the pit bottom, and at the same time, the overlying soil weight could not balance the underlying confined water pressure, the pit bottom may heave and failure can occur. Shown as Fig. 3.37,

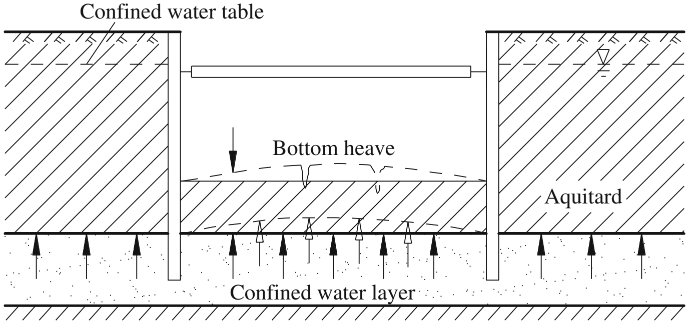

Fig. 3.37 The pit bottom heave induced by confined water pressure

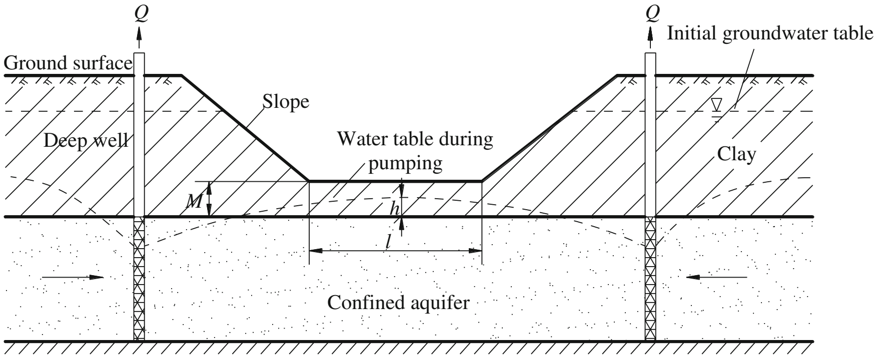

Fig. 3.38 Deep well dewatering

when designing the underground diaphragm wall before construction, the confined water pressure circumstance should be checked; and the stability analysis of the bottom heave can be examined as follows.

Firstly the balance of overlying soil weight and the underlying confined water pressure should be considered. The safety coefficient can be chosen as 1.1–1.3. When this condition could be met, the additional friction force of supporting structure can also be taken into account for the balance, as for the small-scale foundation pit with spatial effect or narrow strip pit. The friction coefficient can be determined according to the specific project by experiments. The earth pressure applied on the supporting structure can use the positive earth pressure for a safe consideration. In addition, the safety factor is taken as 1.2. Hereby if the balance still could not be satisfied, some measurements should be taken to prevent the instability of foundation pit. There are usually two methods:

(1) Underground diaphragm wall to cut off the hydraulic connection of aquifer;
(2) Lowing the confined water pressure by deep well dewatering.

When the thickness of clay layer beneath the pit bottom could not bear the upward confined water pressure, deep well dewatering is usually used to decrease the confined water head to ensure the stability of the pit bottom (Fig. 3.38). Under this circumstance, the stability condition is:

$$\gamma_{\mathrm{w}} \cdot h \leq M \cdot \gamma \tag{3.37}$$

where M is the thickness of clay layer beneath the pit bottom, m; γ is the unit weight of clay layer beneath the pit bottom, kN/m^3; γ_{w} is the unit weight of water, kN/m^3; h is the confined water head after dewatering, m.

3.8.4 The Measurements of Foundation Pit Piping

3.8.4.1 Range of Reinforcement

When the foundation pit encounters piping problems and the dewatering could not be easily used, the soil improvement can be utilized. After the deep geological survey and the calculation analysis on surrounding soil displacement, some rational reinforcement can be pre-conducted on the weak places as for the foundation pit. The required locations and range should be within the following conditions:

1. The clay layer with high thixotropic and rheological properties and the liquid index over 1.
2. Confined aquifer exists below the pit bottom and has large potential to crack the aquitard beneath the pit bottom.
3. Transitional layer of clay aquitard interbedded with confined aquifer exists between the confined aquifer and the pit bottom.
4. Some special external deviator loading conditions on foundation pit:
    (1) Great difference between the surrounding pit surface and groundwater level;
    (2) Some loose soil or cavity exists outside the retaining wall;
    (3) High surcharge loading outside the retaining wall in foundation façade;
    (4) The soil hardness varies a lot from inside to outside of the foundation pit;
    (5) Addition pressure arise due to the adjacent site piling or grouting.
5. Abundant sandy layer with large thickness or water storage body such as abandoned basement pipelines exists.
6. Abundant groundwater with great flow motive connectivity to gravel layer or old building waste layer exists.
7. Some settlement-sensitive construction facilities such as high-rise tower, flammable pipes, underground railway and tunnel exist around the outside of foundation pit.

As for the above adverse circumstances, specific engineering geological and hydrological and the construction conditions should be considered in detail to predict the soil displacement surrounding the foundation pit. After the carefully optimized structure designation of retaining wall, supporting system and excavation technology, if the surrounding soil displacement is still over the allowable deformation amount, some rational soil reinforcement should be considered at some weak stability locations. For the place where the failure potential is really high, the safety factor should be increased accordingly. And grouting in real-time tracking during the excavation can be used to reliably control the differential settlement of protected objects. As for the place where piping and soil erosion may happen, some reliable soil improvement is much more important. The reinforcement place, location, range, and the properties indices after reinforcement should be calculated specifically. Some requirement to check the reinforcement effects needs to be proposed. The reinforcement methods can take the following representative method as reference.

3.8.4.2 Pit Bottom Soil Improvement to Resist the Confined Water Pressure

Piping or bottom heave is the most dangerous problem in foundation pit excavation. When the pit bottom foundation soil could not balance the underlying confined water pressure, some reliable soil improvement should be taken. There are usually three traditional methods as below:

(1) Chemical grouting or high pressure triple jet grouting method. Before excavation, the bottom of underground diaphragm wall is sealed by grouting and connects to the reinforced aquitard layer as a whole mass body to get higher the weight of the overlying soil above the pit bottom. Then it can well balance the underlying confined water pressure (Figs. 3.39 and 3.40). The calculation is seen as Eq. (3.39):

$$h \cdot \gamma_{cp} \geq H \cdot \gamma_w \tag{3.39}$$

where h is the height between the pit bottom to the reinforced soil baseline; γ_{cp} is the mean unit weight above the reinforced soil baseline; $H\gamma_w$ is the confined water pressure.

In the Phase I project of Shanghai combined sewage treatment, the strip deep foundation of Peng-yue-pu Pumping Station is adjacent to some multistory residents' buildings. The total length is 160 m; width is 5.8 m and depth is 15 m. The clay aquitard beneath the pit bottom is only 5 m. It could not bear the underlying 16 t/m^{2}confined water pressure. Then the above recommended method was utilized and the project was completed safely. The excavation in foundation pit of subway

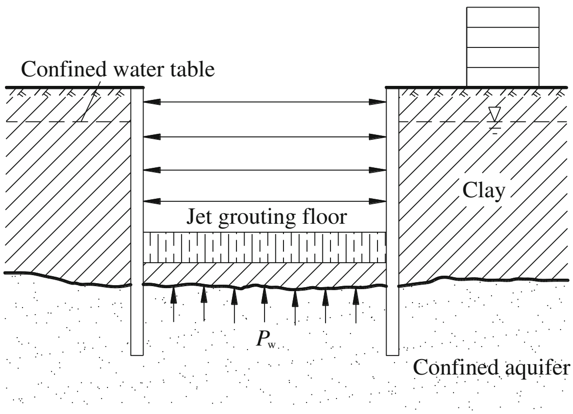

Fig. 3.39 Soil reinforced by jet grouting to resist the confined water pressure

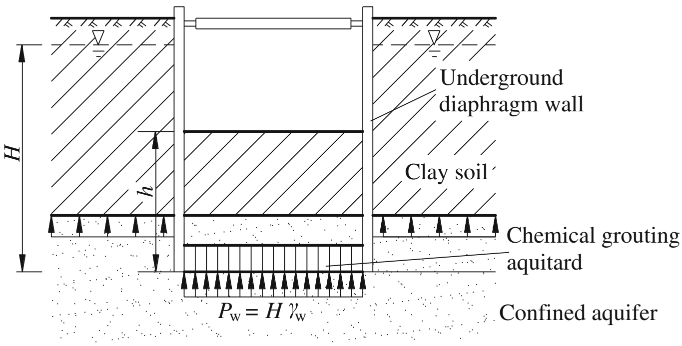

Fig. 3.40 Soil reinforced by chemical grouting to resist the confined water pressure

tunnel in Rotterdam, Netherlands was also applied this method to solve the confined water pressure problem.

(2) Deep well dewatering is conducted inside or outside the foundation pit, and at the same time, recharging is also applied in soil layers of adjacent buildings to control the surrounding settlement. When the foundation pit locates at some open area, recharging is no need (Fig. 3.41).

(3) Sealing curtain is deployed outside the foundation pit. In the loose sand, gravel or high permeability layers under groundwater level, some sealing curtain should be made by mixing piles, jet grouting piles, cement or chemical grouting piles, around the sheet pile retaining wall or outside the poor-sealing wall, to prevent soil erosion and piping at the bottom edge of retaining wall. The imbedded depth of the sealing curtain should meet the requirement of resisting piping (Fig. 3.42).

(4) Pre-consolidation method by dewatering inside the pit. In the high-density urban building area, some dewatering measurements can be taken in the sandy soil

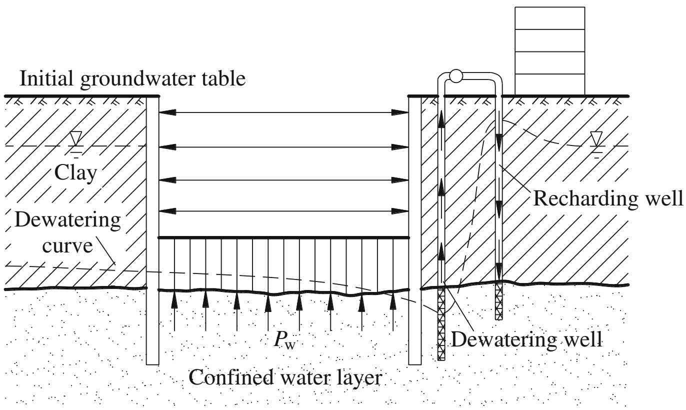

Fig. 3.41 Stabilizing the pit bottom by well dewatering

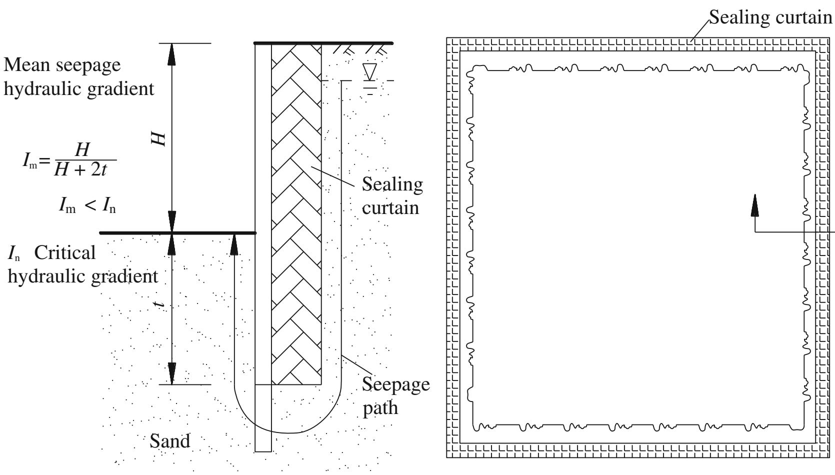

Fig. 3.42 The sealing curtain of retaining wall in foundation pit

or soft clay imbedded with thin sandy layer inside the foundation pit with good sealing curtain wall. Rational wellpoints' arrangement can drain the water in the soils between ground surface and some depth below pit bottom. The pre-dewatering before the pit excavation, can facilitate the soil drainage and consolidation to easy excavation, most importantly resulting in the increase of strength and stiffness, and also decreasing the rheology, to meet the stability and deformation requirement. The time of pre-consolidation is determined by the dewatering depth and the permeability of soils. In the sand imbedded muddy layer of Shanghai, the horizontal coefficient of permeability is about 10^{-4} cm/s. The vertical is smaller than 10^{-6} cm/s. When the dewatering depth is 17–18 m in this layer; and the excavation

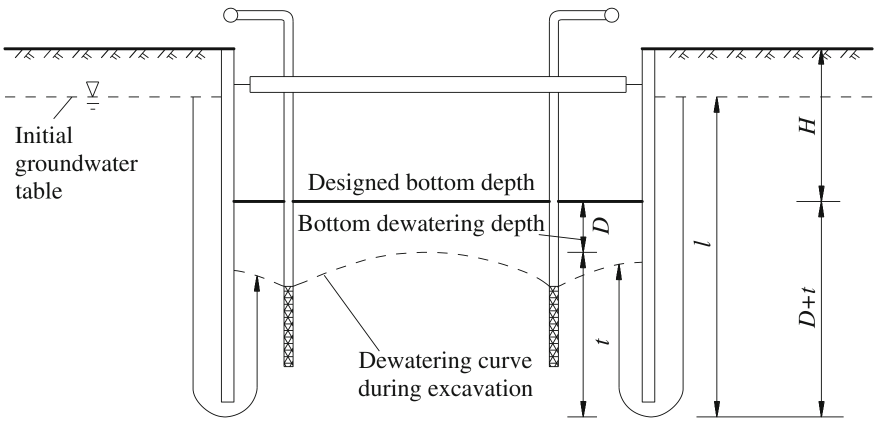

Fig. 3.43 The pre-consolidation by dewatering in foundation pit

duration is 30 d; the pre-consolidation time should be larger than 28 d. In practice, it indicates that the strength of the sand imbedded soft clay layer is augmented by 30 % through the dewatering consolidation. It works more effectively in sandy soils. For better reinforcement effects, the dewatering depth should be checked and rationally determined (Fig. 3.43).

3.9 Exercises

1. Which are the adverse effects of groundwater?
2. What conditions may induce suffosion? How to prevent it?
3. What conditions may induce piping? How to prevent it?
4. What conditions may induce quicksand? How to prevent it?
5. What is the sand liquefaction? What factors may influence it? How to prevent it?
6. What is the mechanism of pore-water pressure influencing on soil strength?
7. What properties of instantaneous stability and long-term stability for saturated clay foundation pit?
8. How groundwater seepage influences the stability of foundation pit or slope?
9. What are the behaviors of piping in foundation pit? How to prevent it?